

Preventing Morphine-Seeking Behavior through the Re-Engineering of Vincamine's Biological Activity

Verrill M. Norwood, IV, Ariana C. Brice-Tutt, Shannel O. Eans, Heather M. Stacy, Guqin Shi, Ranjala Ratnayake, James R. Rocca, Khalil A. Abboud, Chenglong Li, Hendrik Luesch, Jay P. McLaughlin, and Robert W. Huigens, III*

Cite This: *J. Med. Chem.* 2020, 63, 5119–5138

Read Online

ACCESS |



Metrics & More

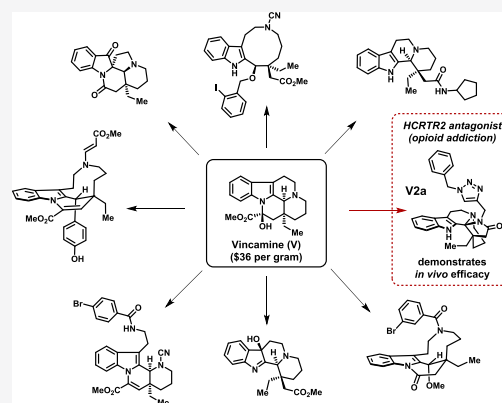


Article Recommendations



Supporting Information

ABSTRACT: Innovative discovery strategies are essential to address the ongoing opioid epidemic in the United States. Misuse of prescription and illegal opioids (e.g., morphine, heroin) has led to major problems with addiction and overdose. We used vincamine, an indole alkaloid, as a synthetic starting point for dramatic structural alterations of its complex, fused ring system to synthesize 80 diverse compounds with intricate molecular architectures. A select series of vincamine-derived compounds were screened for both agonistic and antagonistic activities against a panel of 168 G protein-coupled receptor (GPCR) drug targets. Although vincamine was without an effect, the novel compound **4** (**V2a**) demonstrated antagonistic activities against hypocretin (orexin) receptor 2. When advanced to animal studies, **4** (**V2a**) significantly prevented acute morphine-conditioned place preference (CPP) and stress-induced reinstatement of extinguished morphine-CPP in mouse models of opioid reward and relapse. These results demonstrate that the ring distortion of vincamine offers a promising way to explore new chemical space of relevance to opioid addiction.



INTRODUCTION

An invigorated effort to improve pain management was implemented across the United States (U.S.) in the mid-1990s.¹ Hospitals and inpatient settings began to include “pain scores” as a quality measure for patients. Many clinicians responded to patients’ elevated pain scores by prescribing opioid medications more frequently. Initially, opioid therapies were not believed to be highly addictive; however, we now know that there are significant ramifications associated with opioid misuse as the U.S. is amidst a health-care crisis resulting from opioid addiction and death-related overdoses.^{1–4}

The opioid epidemic has produced devastating public health, social, and economic consequences.^{1–3} Several legal and illegal opioids have played a critical role in the growing crisis and can be categorized as either prescription pain relievers (morphine, codeine, oxycodone), synthetic opioids (fentanyl), or heroin. In 2017, more than 130 people died every day in the U.S. from overdosing on opioids.⁵ According to the National Survey on Drug Use and Health, nearly 12 million individuals in the U.S. misused opioids in 2015.⁶ It is also reported that nearly 80% of heroin users initially misused prescription opioids.⁷ The Center for Disease Control and Prevention estimates the economic burden of prescription misuse alone to be \$78.5 billion each year.² In response to the unprecedented need to treat opioid addiction, there is an increased emphasis to discover new and innovative therapeutic agents for opioid use disorders.

Several natural products have been shown to be excellent starting points for generating diverse and complex compound libraries, which are of importance to those involved in drug discovery.^{8–18} Our group is interested in diverse indole-based compounds,^{14,19} as many are known to bind and modulate an array of therapeutically relevant biological targets, from complex natural products (e.g., vincristine binds microtubules for cancer treatments) to structurally simple synthetic indoles (e.g., ondansetron binds serotonin receptors for nausea therapies).^{19,20} Therefore, we hypothesized that a unique library composed of architecturally diverse indole-based compounds could lead to promising discoveries of relevance to opioid addiction.

Vincamine (**1**) is an indole alkaloid found in the leaves of *Vinca minor* and is available on an affordable decagram scale (~\$36/g). This indole alkaloid is a prescription medicine (Oxybral SR) used to improve cerebral blood flow and cognitive function. Despite vincamine’s interesting biological activity profile, it has no known activities against targets

Received: November 26, 2019

Published: January 8, 2020



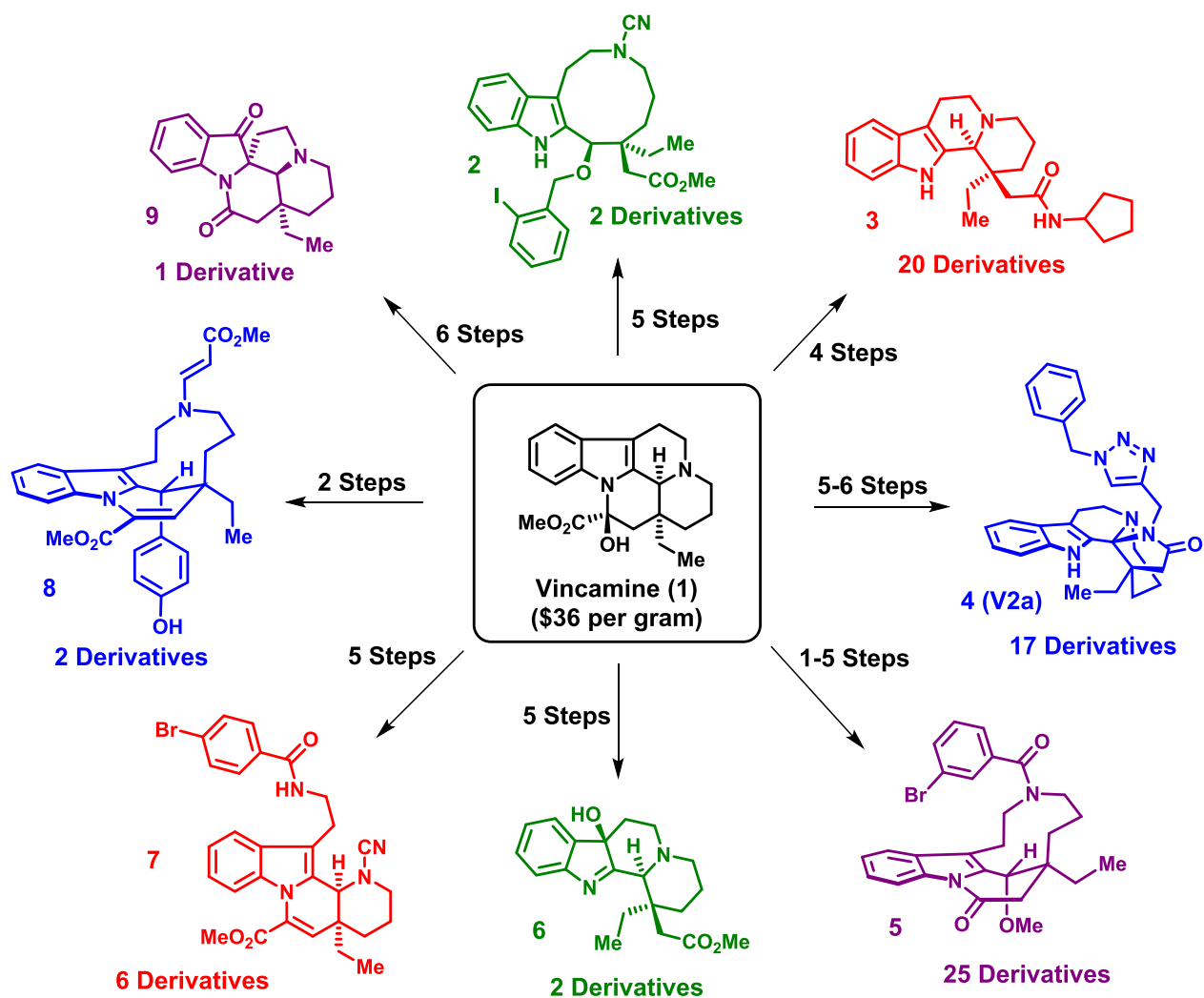


Figure 1. Rapid syntheses of diverse and stereochemically complex molecules from the indole alkaloid vincamine (1).

relevant to opioid addiction; however, we aimed to use vincamine as a starting point to rapidly generate complex and diverse indole-based scaffolds to explore new chemical space through biological screens against a diverse panel of drug targets. The overarching goal of this work is to re-engineer the biological activity of vincamine through dramatic alterations of its inherently complex molecular architecture and identify promising new lead compounds for opioid abuse.

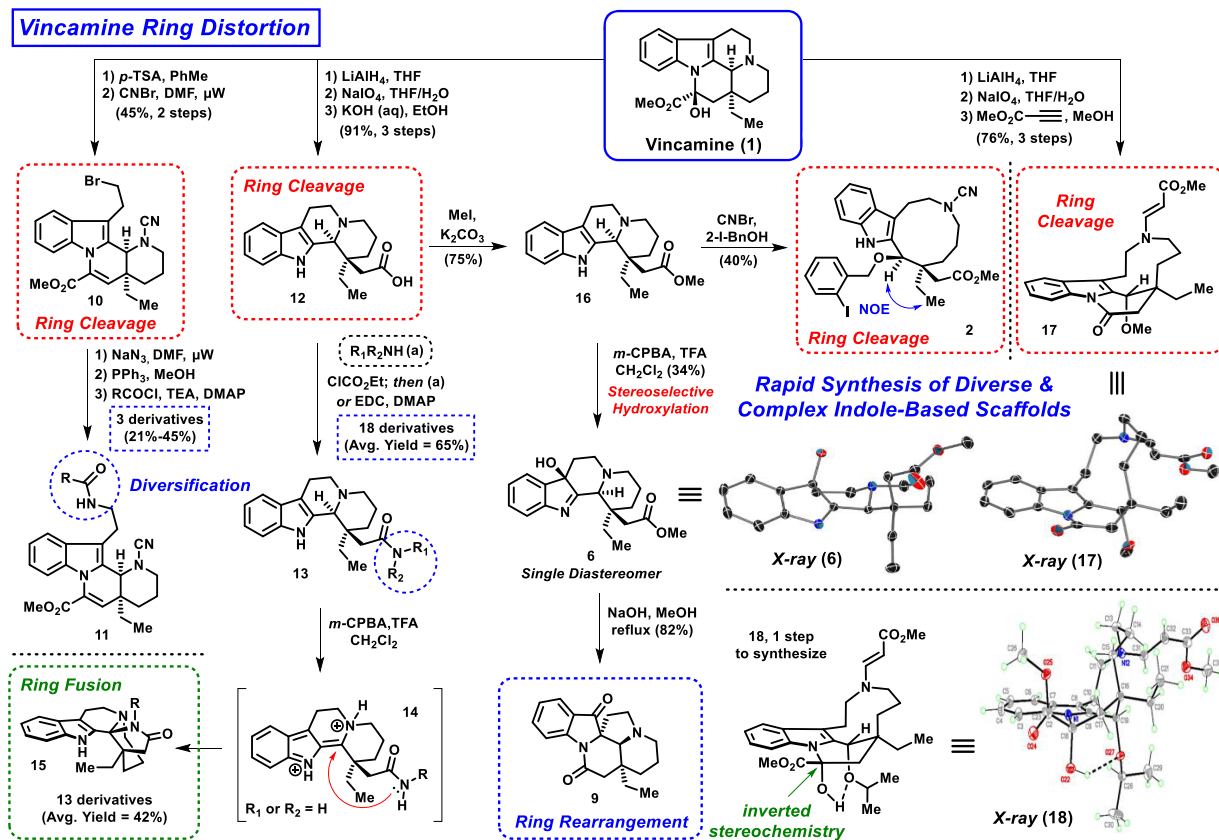
A diverse library of stereochemically complex compounds, with scaffolds related to 2–9 (Figure 1), was rapidly generated in one to six synthetic steps from vincamine using an orchestrated series of chemoselective ring cleavage, ring rearrangement, and ring fusion reactions. Using this ring distortion approach, we synthesized an intricate and diverse library of 80 indole-based small molecules featuring unique and complex molecular architectures (Supporting Information Figures 1 and 2). We evaluated a subset of the library against a panel of 168 G protein-coupled receptor (GPCR) drug targets, several of which demonstrated activity profiles distinct from vincamine and other complex, indole-based small molecules synthesized during these investigations.

RESULTS AND DISCUSSION

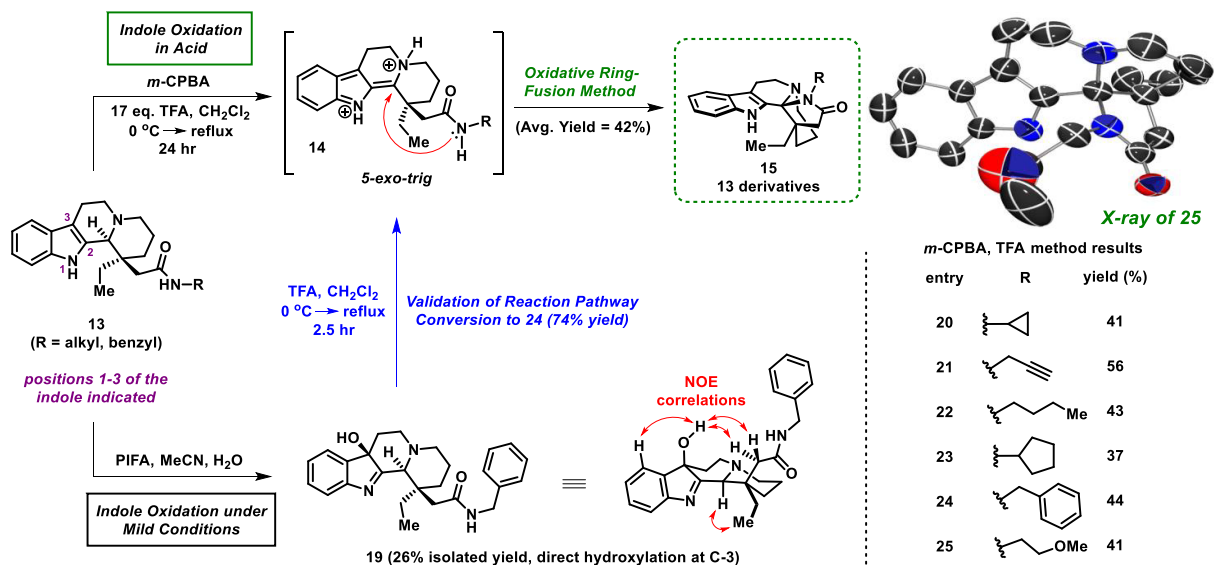
Ring Distortion of Vincamine To Rapidly Generate Diverse, Stereochemically Complex Indole-Based Com-

pounds. Following an initial query of the literature, we identified two ring cleavage transformations from vincamine that were useful during our ring distortion efforts.^{21,22} We developed a modified version of the first ring cleavage²¹ to afford **12**, which is a three-step synthesis from vincamine using (1) lithium aluminum hydride, (2) sodium periodate, and then (3) potassium hydroxide (91% yield/three steps; ≥ 3.5 g for each step; Scheme 1). The second ring cleavage reaction from vincamine utilizes methyl propiolate in methanol to afford structures similar to **17** as a single diastereomer.²² In this reaction, the tertiary amine of vincamine undergoes a conjugate addition to methyl propiolate, in turn, activating the C–N bond adjacent to the indole heterocycle for ring cleavage. We used various alcohol solvents as nucleophiles to attack the carbon adjacent to the 2-position of the indole heterocycle, which occurs with complete inversion of stereochemistry. We found sterically encumbered alcohol nucleophiles to induce a stereoinversion of the α -hydroxyester center in vincamine during this reaction. Presumably, stereoinversion occurs through a ring-opening and -closing pathway to furnish **18** and related analogues. An interesting feature of **18** is the hydrogen-bonding interaction between the inverted hydroxyl and resultant isopropyl ether oxygen atom that can be seen in the X-ray structure of **18** (Scheme 1). We believe that this stereoinversion is favored and occurs to avoid steric

Scheme 1. Ring Distortion of Vincamine Enables the Rapid Generation of Complex Compounds for Biological Investigations



Scheme 2. Novel Oxidative Cyclization Method from Amides (13) to Ring Fusion Analogues of 15 with Mechanistic Validation Involving Critical Compound 19



interactions between bulky ether groups and the methyl ester that would be on the same face in the resulting products. In addition, this ring cleavage reaction is applicable to several vincamine-derived substrates.

In addition, cyanogen bromide (CNBr) was utilized for regioselective C–N ring cleavage reactions, similar to our previous studies with yohimbine.¹⁴ Compound 16 was treated with cyanogen bromide and 2-iodobenzyl alcohol to afford

indole-promoted C–N ring cleavage product 2 in a 40% yield as a single diastereomer. Alternatively, a von Braun reaction that occurs through a second-order nucleophilic substitution (S_N2) pathway can be employed utilizing cyanogen bromide in *N,N*-dimethylformamide (DMF) under microwave conditions to yield alternative ring cleavage scaffold 10 (45% yield, two steps), which was elaborated into a series of amide analogues 11.

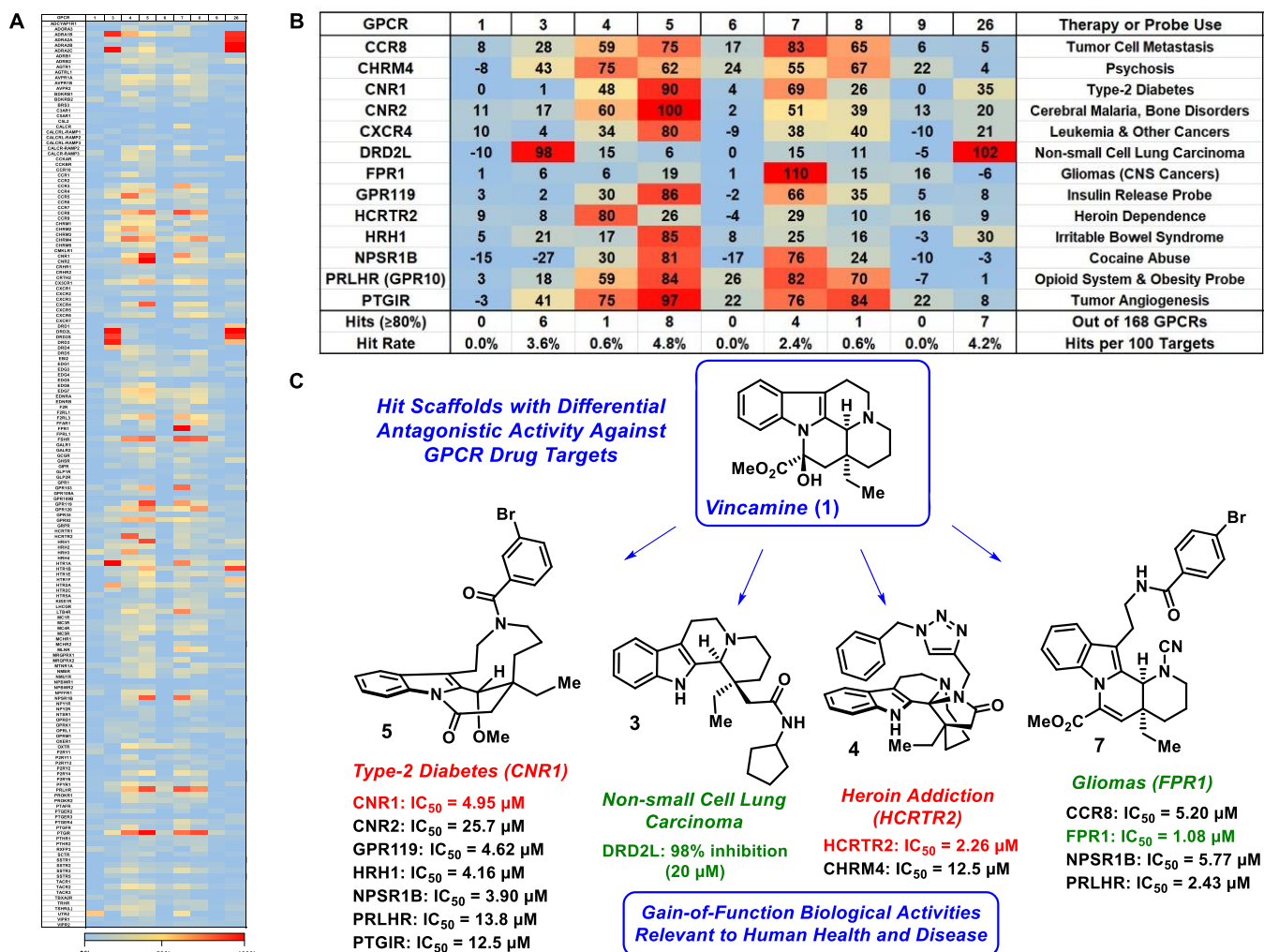


Figure 2. GPCR screening results (heatmaps) with therapeutic and probe applications for vincamine ring distortion compounds 3–5, 7, and 8. (A) Antagonistic activity heatmap of 168 GPCR panel against vincamine, yohimbine, and tested vincamine ring distortion compounds. (B) Focused heatmap of hit compounds and antagonistic activities against GPCRs of interest in medicine. (C) Active compounds 3–5, and 7 display differential GPCR activity profiles compared to vincamine (1) and other ring distortion compounds.

During this study, we found 12 to be an excellent starting point for innovative and provocative ring distortion reactions. One of our synthetic goals was to carry out the selective oxidation of the indole nucleus upon treatment with *meta*-chloroperbenzoic acid (*m*-CPBA) to afford C-3 hydroxylated products (e.g., 6).^{19,23} The hydroxylation of indoles at C-3 provides a synthetic opportunity to access interesting ring rearrangement scaffolds from vincamine following a base-promoted 1,2-alkyl shift to afford spiro-3-oxindoles. During these studies, 16 was stereoselectively hydroxylated with *m*-CPBA and trifluoroacetic acid (TFA; Scheme 1) in methylene chloride to afford 6 as a single diastereomer in a 34% yield (axially protonated amine of 16 hydrogen bond directs *m*-CPBA;²⁵ β -hydroxylation affords 6; see X-ray). Subsequent exposure of 6 to sodium hydroxide induced a semipinacol rearrangement to furnish spiroindoxyl 9 in an 82% yield.

The carboxylic acid of 12 readily undergoes amidation reactions using ethyl chloroformate, or 1-ethyl-3-(3-dimethylaminopropyl)carbodiimide (EDC) with catalytic 4-dimethylaminopyridine (DMAP), followed by the addition of diverse amines to afford 13 (18 amide derivatives, 65% average yield; Scheme 1). In contrast to the hydroxylation of the indole nucleus (e.g., conversion of 16 to 6), we discovered that amide

analogues (13) undergo an intriguing oxidative ring fusion reaction upon treatment with *m*-CPBA and TFA (Schemes 1 and 2). Surprisingly, no C-3 hydroxylated products were observed upon treatment of amides 13 with *m*-CPBA and TFA; however, this transformation was robust and afforded 13 unique ring-fused analogues of 15 in a 31–56% yield (42% average yield). Rationalizing the reaction mechanism for the oxidative ring fusion was an initial challenge. However, we hypothesized that *m*-CPBA initially reacts with the indole of 13 to give the expected 3-hydroxyindolenine intermediate. Then, we proposed that TFA (17 equiv) under refluxing conditions leads to a subsequent elimination (dehydration), resulting in intermediate 14, which undergoes a final 5-exo-trig cyclization between the amide nitrogen (nucleophile) and the resonance-stabilized carbocation adjacent to the C-2 position of the indole heterocycle, rationally leading to the observed ring-fused scaffolds (15).

To test our hypothesis regarding the mechanism of the oxidative ring fusion reaction (conversion of 13 to 15), we utilized the hypervalent iodine reagent [bis(trifluoroacetoxy)iodo]benzene (PIFA) and water as a milder oxidizing system²⁴ to isolate desired C-3 hydroxylated 19 (Scheme 2) in a 26% yield. 19 is an important intermediate regarding our proposed

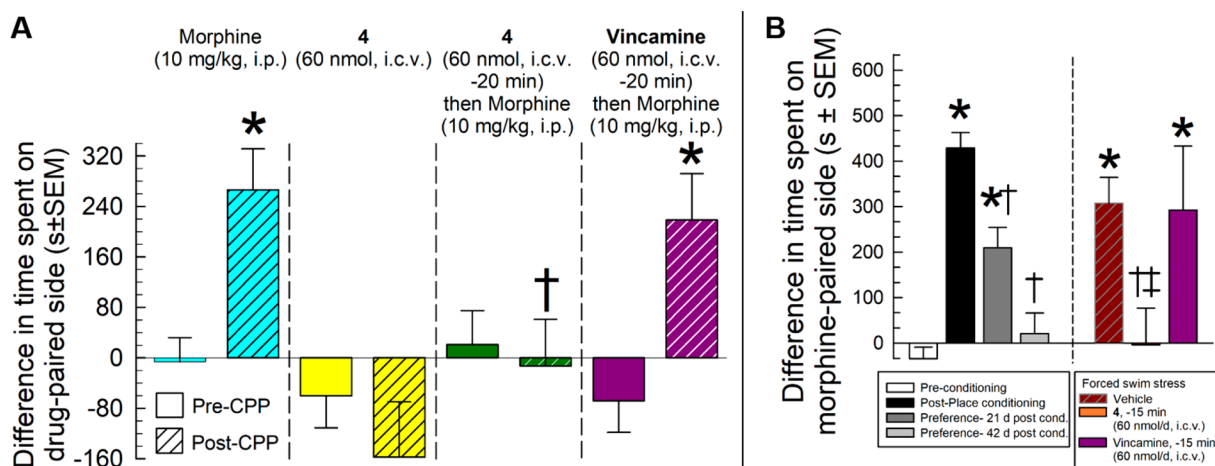


Figure 3. Results of **4** (V2a) and vincamine in morphine-CPP studies in mouse models of opioid reward and relapse. (A) **4** pretreatment prevents morphine-conditioned place preference (CPP) in mice. In place conditioning, mice exhibited significant morphine-CPP (left bars), but **4** (60 nmol, i.c.v.) did not significantly differ from initial preferences (center bars). **4**, but not vincamine, pretreatment 20 min prior to morphine significantly prevented morphine-CPP. $n = 16\text{--}30$ mice/group. *, $p < 0.05$ vs preconditioning response; †, $p < 0.05$ vs morphine-CPP, Tukey post hoc test. (B) Stress-induced reinstatement of morphine-CPP in mice prevented by **4** pretreatment. Mice exhibited significant morphine-CPP, with extinction occurring by 7 weeks (left bars). Forced swimming (right bars) reinstated place preference in vehicle or vincamine-treated mice. **4** pretreatment prevented stress-induced reinstatement. $n = 16\text{--}21$ mice/group; 58 mice total. *, $p < 0.05$ vs preconditioning response (leftmost bar); †, $p < 0.05$ vs post CPP (second bar on left); ‡, $p < 0.05$ vs stress-induced reinstatement (striped red bar, center), Tukey's post hoc test.

reaction mechanism that leads to the formation of ring fusion analogues (**15**). Upon exposure of **19** to TFA (without *m*-CPBA) in refluxing methylene chloride, we were delighted to see the rapid formation of ring fusion compound **24** in a 74% yield in 2.5 h (Scheme 2; the X-ray of analogue **25** confirms C–N bond formation upon ring closure). These findings support our proposed mechanism regarding the conversion of amides (**13**) to novel ring fusion analogues (**15**).

Biological Evaluation against a Diverse Panel of GPCR Drug Targets. Following synthesis, seven unique vincamine-derived compounds were selected to represent a maximal chemical diversity from the synthesized library (analogues **3–9**; one from each of the distinct scaffold types from vincamine; chemoinformatic analyses of vincamine-derived analogues can be seen in the Supporting Information Figure 6) and screened against a panel of 168 G protein-coupled receptor (GPCR) drug targets in cell-based assays (Figure 2; Supporting Information Figures 3 and 4).²⁵ Each compound was screened at 20 μM for agonist and antagonist activities against the GPCR panel, which contained targets relevant to opioid addiction (e.g., opioid receptors OPRM1, OPRD1, OPRK1, OPRK2; cannabinoid receptor 1 CNR1²⁶ and hypocretin receptor HCRTR2²⁷). In addition, parent vincamine and comparator indole alkaloid yohimbine (**26**) were screened alongside the new synthetic analogues. We hypothesized that indole-based compounds with diverse molecular architectures would lead to new and exciting hit compounds that demonstrate GPCR activity profiles distinct from each other and the parent vincamine.

Although minimal agonistic activity was found in this screen, differential profiles were obtained in the antagonism mode. The GPCR antagonists were indeed distinct from vincamine's activity profile ($\geq 80\%$ inhibition was considered to be a "hit" in this screen; Figure 2). Vincamine demonstrated no antagonistic activities against this panel of GPCRs; however, five of the seven diverse, ring-distorted compounds reported at least one GPCR hit, including **3** (six hits, 3.6% hit rate), **4** (one hit, 0.6% hit rate), **5** (eight hits, 4.8% hit rate), **7** (four hits, 2.4% hit

rate), and **8** (one hit, 0.6% hit rate). As a comparator in this screen, yohimbine (**26**; indole alkaloid) was shown to antagonize seven GPCRs (4.2% hit rate) that include adrenergic, dopamine, and serotonin receptors, which has previously been reported in the literature.²⁸

The "gain-of-function" GPCR antagonistic activities regarding **3–5**, **7**, and **8** compared to vincamine were the initial proof-of-concept result that our ring distortion approach could lead to molecules with re-engineered biological activities (based on a $>70\%$ differential antagonistic activity in screen comparing vincamine to ring distortion analogues). Concentration–response experiments were subsequently performed with select compounds (**4**, **5**, **7**) for antagonistic activities against specific GPCRs. These experiments allowed for the determination of potency for analogues **4**, **5**, and **7** against relevant GPCRs, resulting in several IC_{50} values in the low micromolar range.

Following initial screens, we turned our attention to analogue **4** (V2a), which demonstrates antagonistic activity against hypocretin (orexin) receptor 2 (HCRTR2; $\text{IC}_{50} = 2.26 \mu\text{M}$; Figure 2). We were encouraged by initial results, as hypocretin receptor 2 antagonism recently demonstrated a dose-dependent reduction of heroin self-administration in rats.²⁷ In addition, analogue **4** demonstrated a good selectivity profile for targeting HCRTR2 in the GPCR panel, including no significant modulatory activities ($<20\%$) of opioid receptors at 20 μM .

Stability concerns regarding the potential acid-labile *N,N'*-carbon (sp^3) center adjacent to the 2-position of the indole nucleus of **4** were probed experimentally. Encouragingly, we found that **4** could be readily interconverted to the corresponding HCl salt (of the basic amine) and free base forms under mild experimental conditions (see the Supporting Information for HCl salt and free base of **4**, including NMR spectra). In addition, analogue **4** proved to have robust acid stability following 24 h exposure to acidic media at 37 $^{\circ}\text{C}$ (92.1% recovery in pH 2.0; 99.2% recovery in pH 4.88; Supporting Information). With the selective HCRTR2 antagonistic activity and chemical stability results in hand, we

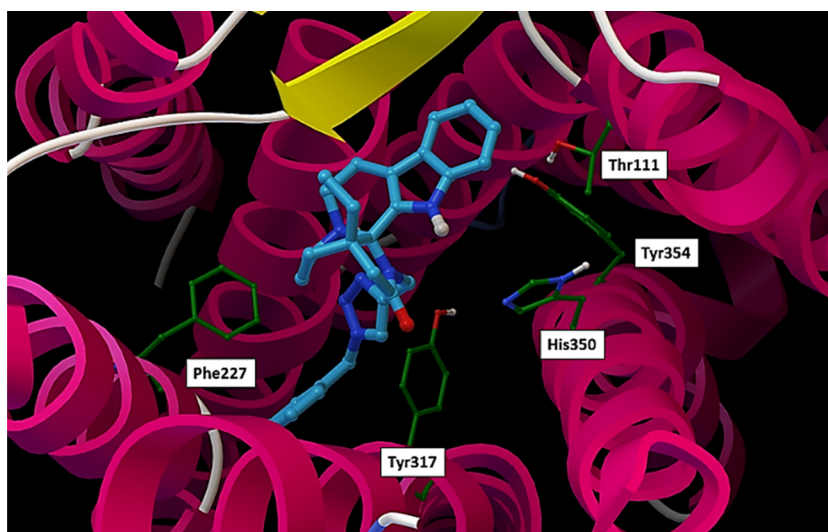


Figure 4. Molecular modeling of 4 (V2a) bound to HCRTR2. (Note: PDB ID 4S0V.).

were curious to know if 4 could attenuate opioid-seeking in mouse models using behavioral pharmacological approaches.

Animal Studies To Determine the Efficacy of 4 (V2a) in Morphine-Seeking Mouse Models. We evaluated 4 (V2a) to determine the potential for this novel compound to prevent acute morphine-conditioned place preference (CPP) and stress-induced reinstatement of extinguished morphine-CPP in mice. A major problem in treating individuals with opioid addiction is the occurrence of relapse, which is often caused by a stressful event.^{29–31} For humans, examples of stressful life events that could lead to relapse (reinstatement) include the loss of employment or a relationship; however, in reinstatement experiments in the lab, mice are subjected to a forced swim test (FST) that triggers a stress response that leads to subsequent morphine-seeking behaviors.

In counterbalanced conditioned place preference experiments in mice,^{32–36} intracerebroventricular (i.c.v.) treatment of 4 was without a significant effect alone, but a 20 min pretreatment prior to conditioning prevented acute morphine-CPP [two-way analysis of variance (ANOVA), $F_{(3,170)} = 4.65$, $p = 0.004$; Figure 3A]. A similar pretreatment with the parent vincamine was without a significant effect on morphine-CPP (final preference, 219 ± 74 s, $p = 0.998$ vs morphine-CPP, Tukey's post hoc test), further suggesting that the effects of 4's in vivo efficacy are due to HCRTR2 antagonism. Pretreatment with 4 also significantly prevented stress-induced reinstatement of extinguished morphine-seeking behavior (one-way ANOVA, $F_{(6,281)} = 9.76$, $p < 0.0001$; Figure 3B) compared to that of a vehicle control in mice subjected to a forced swim test, whereas vincamine did not. Combined, this data clearly indicates that ring distortion can be used to re-engineer vincamine's biological activity and 4 holds promise for further exploration as a potential treatment for opioid abuse.

Molecular Modeling of 4 (V2a) in HCRTR2. We used molecular modeling to determine a binding mode of 4 (V2a) in the antagonistic binding site of HCRTR2. Our goal was to establish a rational design pathway for future development efforts. Initially, we docked the HCRTR2 antagonists suvorexant and EMPA to their respective binding conformations (suvorexant to PDB ID 4S0V;³⁷ EMPA to PDB ID SWQC³⁸). The redocking of these antagonists using Glide XP and AutoDock4 generated binding poses close to crystallo-

graphic binding modes with both root-mean-square deviation (RMSD) less than 1.0 Å, whereas redocking using Glide SP could not find the crystallographic binding modes with both RMSD larger than 7.0 Å. Therefore, we found our customized docking protocols with Glide XP and AutoDock4 to be better than Glide SP scoring, which was reasonable as the binding site of HCRTR2 is relatively closed with a deep binding cleft. When compound 4 was docked to both modeled conformations, we found the 4S0V conformation to be significantly better than SWQC, since using a 1.5 Å RMSD threshold, 4S0V, yields an 11% conformational clustering with -10.2 kcal/mol calculated binding energy whereas SWQC yields a 4% conformational clustering with -9.1 kcal/mol. This result made sense, as suvorexant has structural similarities to 4.

The binding mode of 4 (V2a) to HCRTR2 matches that of suvorexant at several corresponding functional groups/fragments, which include (1) the indole group of 4 to the benzoxazole group of suvorexant, (2) azacyclohexyl to diazepam, and (3) triazole to triazole (see the Supporting Information Figure 5). A major difference is that the terminal benzyl group of 4 binds deeply into an extra subpocket of HCRTR2 (binding model seen in Figure 4). The indole of 4 binds at a major hydrophobic region (major residues of Pro131, Cys107, and Val138, not shown for clarity). The triazole of 4 has an aromatic interaction with Tyr317, the same for the terminal benzene with Phe227. Collectively, our data suggests that 4 is an ideal template to develop improved HCRTR2 antagonists using molecular modeling to rationally design new agents to treat opioid abuse.

CONCLUSIONS

In conclusion, we have synthesized a diverse collection of complex compounds from vincamine bearing distinct molecular architectures. During these investigations, we discovered a novel oxidative ring fusion reaction that led to the discovery of 4 (V2a), which demonstrates HCRTR2 antagonistic activities. As HCRTR2 was recently reported to be relevant in heroin addiction,²⁷ 4 was advanced to animal studies and demonstrated in vivo efficacy in acute and reinstatement mouse models of morphine reward. In addition, we established a model for 4 binding to HCRTR2 using molecular docking, which will be utilized to direct future analogue design and

synthesis. These findings further support the therapeutic potential of HCRTR2 antagonists to treat opioid abuse. Finally, this work demonstrates the significant potential ring distortion has in re-engineering the biological activity of natural products, such as vincamine, for new applications of critical importance to human health.

EXPERIMENTAL SECTION

General Information. The purities of all compounds evaluated in biological assays were confirmed to be $\geq 95\%$ by liquid chromatography–mass spectrometry (LC–MS) using a Shimadzu Prominence high-performance liquid chromatography (HPLC) system, an AB Sciex 3200 QTRAP spectrometer, and a Kinetex EVO C18 column (50 mm \times 2.1 mm \times 2.6 μm) with a 30 min linear gradient from 30 to 95% acetonitrile in 5 mM ammonium bicarbonate at a flow rate of 0.25 mL/min. All GPCR screens and concentration-dependent experiments were conducted at DiscoverX (<https://www.discoverx.com/arrestin>). All animal experiments were carried out at the University of Florida and authorized by the Institutional Animal Care and Use Committee (IACUC) under protocol 201910772. The University of Florida's accreditation number for animal welfare work is A3377-01. The University of Florida also holds continuous accreditation from AAALAC since 1960.

Chemistry. All reactions were carried out under an atmosphere of argon unless otherwise specified. Chemical reagents were purchased from commercial sources and used without further purification. Vincamine was purchased from AK Scientific at $>98\%$ purity ($\sim \$36 \text{ g}^{-1}$ during these studies). Anhydrous solvents were transferred via syringe to flame-dried glassware, which was cooled under a stream of dry argon. All microwave reactions were carried out in sealed tubes in an Anton Paar Monowave 300 microwave synthesis reactor. Constant power was applied to ensure reproducibility. Temperature control was automated via an IR sensor, and all indicated temperatures correspond to the maximal temperature reached during each experiment. Analytical thin-layer chromatography (TLC) was performed using 250 μm silica gel 60 F₂₅₄ precoated plates (EMD Chemicals Inc.). Flash column chromatography was performed using a 230–400 mesh 60 Å silica gel (Sorbent Technologies).

NMR experiments were recorded on the following instruments: Varian Unity spectrometer (400 MHz for ^1H NMR; 100 MHz for ^{13}C NMR), Bruker Avance III spectrometer (500 MHz for ^1H NMR; 125 MHz for ^{13}C NMR), Bruker Avance II spectrometer (600 MHz for ^1H NMR; 150 MHz for ^{13}C NMR), and Agilent Systems VNMR spectrometer (600 MHz for ^1H NMR; 150 MHz for ^{13}C NMR). All spectra are presented using MestReNova 11.0 (Mnova) software and are displayed without the use of the signal suppression function. Spectra were obtained in the following solvents (reference peaks included for ^1H and ^{13}C NMRs): CDCl_3 (^1H NMR: 7.26 ppm; ^{13}C NMR: 77.23 ppm), deuterated dimethyl sulfoxide ($\text{DMSO}-d_6$) (^1H NMR: 2.50 ppm; ^{13}C NMR: 39.52 ppm), CD_3CN (^1H NMR: 1.94 ppm; ^{13}C NMR: 1.32 ppm), and $\text{CD}_3\text{OD}-d_4$ (^1H NMR: 3.31 ppm; ^{13}C NMR: 49.00 ppm). NMR samples where the respective solvent peaks were buried in the sample signals referenced tetramethylsilane (TMS) at 0.00 ppm for ^1H NMR experiments. NMR experiments were performed at room temperature unless otherwise indicated. Chemical shift values (δ) are reported in parts per million (ppm) for all ^1H NMR and ^{13}C NMR spectra. ^1H NMR multiplicities are reported as: s = singlet, d = doublet, t = triplet, q = quartet, p = pentet, m = multiplet, br = broad.

Select compounds are presented in this section with key signals used for characterization. Compound structures were converted into IUPAC names using MarvinSketch (ChemAxon; Cambridge, MA). Melting points were obtained on a Mel-Temp II capillary melting point apparatus and were uncorrected. High-resolution mass spectra were obtained from the Mass Spectrometry Facility in the Chemistry Department at the University of Florida (UF).

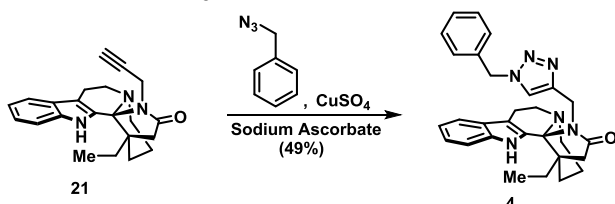
Synthesis Procedure for the Generation of 2, Methyl 2-[(7S,8R)-3-Cyano-7-ethyl-8-[(2-iodophenyl)methoxy]-1H,2H,3H,4H,5H,6H,7H,8H,9H-azecino[5,4-b]indol-7-yl]acetate.

Compound 16 (179 mg, 0.549 mmol) was added to a round-bottom flask and dissolved in chloroform (11 mL). To the resulting solution was added 2-iodobenzyl alcohol (374 mg, 1.60 mmol), and then a 3.0 M solution of cyanogen bromide (0.137 mL, 0.412 mmol in dichloromethane) was added dropwise at room temperature. The reaction was allowed to stir for 25 h and, upon completion (by TLC), quenched with brine, extracted with dichloromethane, and the organic layer was dried with sodium sulfate. The organic layer was then filtered, concentrated in vacuo, and the crude material was purified via column chromatography 100% hexanes to 3:2 hexanes/ethyl acetate to afford 2 (130 mg, 40%) as a yellow-brown residue. ^1H NMR: (500 MHz, CDCl_3 , at 50 $^\circ\text{C}$) δ 10.07 (s, 1H), 7.80 (d, $J = 7.9$ Hz, 1H), 7.51 (d, $J = 7.9$ Hz, 1H), 7.48 (d, $J = 8.2$ Hz, 1H), 7.30 (dd, $J = 8.2, 7.5$ Hz, 1H), 7.26–7.18 (m, 2H), 7.13 (dd, $J = 8.3, 7.5$ Hz, 1H), 6.96 (td, $J = 7.6, 1.8$ Hz, 1H), 4.54 (s, 1H), 4.24 (d, $J = 11.6$ Hz, 1H), 4.13 (d, $J = 11.6$ Hz, 1H), 3.70 (m, 1H), 3.58 (m, 1H), 3.54 (s, 3H), 3.21 (dt, $J = 15.4, 3.3$ Hz, 1H), 3.14 (dt, $J = 14.2, 4.9$ Hz, 1H), 3.01–2.92 (m, 2H), 2.45 (d, $J = 13.3$ Hz, 1H), 2.37 (m, 1H), 2.31 (d, $J = 13.4$ Hz, 1H), 1.65–1.40 (m, 4H), 1.31 (m, 1H), 0.99 (t, $J = 7.5$ Hz, 3H). ^{13}C NMR: (100 MHz, CDCl_3 , at 50 $^\circ\text{C}$) δ 174.7, 140.3, 139.6, 136.4, 132.9, 130.4, 129.7, 128.2, 127.4, 122.8, 119.7, 119.6, 118.4, 112.2, 111.9, 99.3, 78.8, 75.2, 53.6, 53.0, 51.8, 46.0, 38.3, 30.7, 26.9, 26.2, 23.7, 8.2. High-resolution mass spectrometry (HRMS) [electrospray ionization (ESI)]: calcd for $\text{C}_{28}\text{H}_{32}\text{IN}_3\text{O}_3\text{Na}$ [$M + \text{Na}$] $^+$: 432.2258, found: 432.2261. $[\alpha]_{\text{D}}^{20}$: -23° (c 0.10 g/100 mL, MeOH). Note: the stereochemistry of 2 was determined using one-dimensional (1-D) nuclear Overhauser enhancement spectroscopy (NOESY) (see NMR spectrum; Supporting Information).

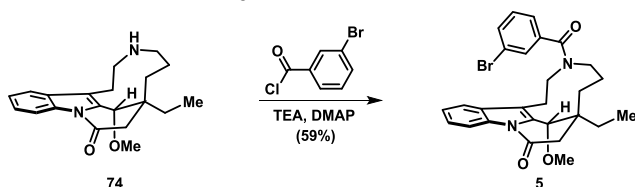
Synthesis Procedure for the Generation of 3, 2-[(1S,12bS)-1-Ethyl-1H,2H,3H,4H,6H,7H,12H,12bH-indolo[2,3-a]quinolinin-1-yl]-N-cyclopentylacetamide. Compound 12 (138 mg, 0.441 mmol) was added to a flame-dried round-bottom flask and dissolved in anhydrous dichloromethane (4.5 mL). The reaction was cooled to 0 $^\circ\text{C}$, and triethylamine (89 μL , 0.882 mmol) was added dropwise. After stirring for 5 min, ethyl chloroformate (47 μL , 0.485 mmol) was added, and the reaction continued to stir for an additional 30 min. Cyclopentylamine (0.435 mL, 4.41 mmol; 0.3 M in dichloromethane) and 4-dimethylaminopyridine (DMAP, one crystal) in anhydrous dichloromethane were then added to the reaction mixture, which was allowed to slowly warm to room temperature. The reaction was continued to stir for 3 h and, upon completion (monitored by thin-layer chromatography, TLC), quenched with brine. The crude reaction mixture was extracted with dichloromethane, dried with sodium sulfate, filtered, and the organic layer was concentrated in vacuo. The crude product was then purified via column chromatography using a gradient of 99:1 hexanes/triethylamine to 74.5:24.5:1 hexanes/ethyl acetate/triethylamine to afford 3 (152 mg, 91%) as a yellow-white solid. ^1H NMR: (600 MHz, CDCl_3) δ 7.93 (s, 1H), 7.46 (d, $J = 7.9$ Hz, 1H), 7.33 (d, $J = 7.7$ Hz, 1H), 7.15 (dd, $J = 8.3, 7.5$ Hz, 1H), 7.09 (dd, $J = 8.2, 7.2$ Hz, 1H), 5.41 (s, 1H), 3.84 (m, 1H), 3.35 (s, 1H), 3.05–2.90 (m, 2H), 2.89 (m, 1H), 2.72–2.53 (m, 2H), 2.40 (dd, $J = 14.4, 11.7$ Hz, 1H), 2.12–2.01 (m, 2H), 2.00–1.87 (m, 3H), 1.81 (m, 1H), 1.68–1.36 (m, 8H), 1.18 (t, $J = 7.6$ Hz, 3H), 1.15 (m, 1H), 0.97 (m, 1H). ^{13}C NMR: (150 MHz, CDCl_3) δ 172.0, 136.2, 133.3, 126.8, 121.9, 119.7, 118.1, 111.9, 111.1, 66.8, 57.1, 54.3, 51.2, 41.0, 40.6, 33.5, 33.1, 32.8, 31.7, 23.8, 23.8, 22.4, 22.1, 8.3. HRMS (ESI): calcd for $\text{C}_{24}\text{H}_{34}\text{N}_3\text{O}$ [$M + \text{H}$] $^+$: 380.2696, found: 380.2710. MP: 64–66 $^\circ\text{C}$. $[\alpha]_{\text{D}}^{20}$: -45° (c 0.11 g/100 mL, MeOH). Note: N-cyclopentylbenzamide was synthesized to assist with the characterization of the aliphatic region of 3 (Supporting Information).

Synthesis Procedure for the Generation of 4, (1S,17S)-20-[(1-Benzyl-1H-1,2,3-triazol-4-yl)methyl]-17-ethyl-3,13,20-triazapentacyclo[11.7.0.0^{1,17}.0^{2,10}.0^{4,9}]icosa-2(10),4,6,8-tetraen-19-one. Anhydrous copper sulfate (66.4 mg, 0.42 mmol) and sodium ascorbate (258 mg, 1.3 mmol) were added to a round-bottom flask and dissolved in a solution of *tert*-butanol/water (1:2, 30 mL). Alkyne-containing compound 21 (307 mg, 0.884 mmol) was added, then benzyl azide (332 μL , 2.7 mmol) as a solution in dichloromethane (2 mL) was added, and the reaction was stirred for 1 h at room temperature, before heating to 30 $^\circ\text{C}$ and allowed to stir for an

additional 14 h. Upon completion (by TLC), the reaction was quenched with brine, extracted with dichloromethane, and the organic layer was dried with sodium sulfate. The organic layer was filtered, concentrated in vacuo, and the crude material was purified via column chromatography using a gradient of 99:1 hexanes/triethylamine to 24.5:74.5:1 hexanes/dichloromethane/triethylamine. Following the column, the compound was dissolved in chloroform and washed with deionized water to afford **4** (210 mg, 49%) as a yellow solid. $^1\text{H NMR}$: (500 MHz, CDCl_3) δ 9.13 (s, 1H), 7.40 (d, J = 8.9 Hz, 2H), 7.21–7.14 (m, 2H), 7.10–7.04 (m, 3H), 6.78 (s, 1H), 6.73 (d, J = 6.7 Hz, 2H), 4.68 (d, J = 14.7 Hz, 1H), 4.55 (d, J = 15.1 Hz, 1H), 4.09 (d, J = 15.1 Hz, 1H), 4.05 (d, J = 14.9 Hz, 1H), 3.36 (dt, J = 12.0, 6.3 Hz, 1H), 3.27 (dt, J = 11.8, 4.8 Hz, 1H), 3.02–2.88 (m, 3H), 2.70–2.58 (m, 2H), 2.24 (d, J = 16.9 Hz, 1H), 2.03 (dt, J = 13.8, 4.0 Hz, 1H), 1.77 (m, 1H), 1.57 (sextet, J = 7.4 Hz, 1H), 1.44 (td, J = 13.1, 3.7 Hz, 1H), 1.37–1.20 (m, 2H), 0.80 (t, J = 7.4 Hz, 3H). $^{13}\text{C NMR}$: (100 MHz, CDCl_3) δ 173.7, 143.1, 137.2, 134.7, 133.0, 128.9, 128.6, 127.9, 126.2, 122.4, 121.6, 119.4, 118.7, 114.0, 111.9, 82.7, 52.9, 50.2, 49.8, 44.7, 43.6, 35.3, 32.4, 25.9, 21.8, 17.8, 9.6. HRMS (ESI): calcd for $\text{C}_{29}\text{H}_{33}\text{N}_6\text{O}$ [$\text{M} + \text{H}$] $^+$: 481.2710, found: 481.2731. MP: 83–85 °C. $[\alpha]_{\text{D}}^{20}$: +102° (c 0.10 g/100 mL, MeOH).



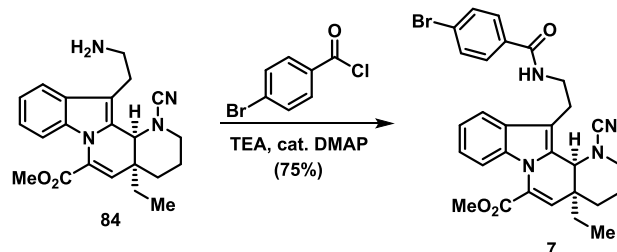
Synthesis Procedure for the Generation of 5, (11S,19R)-15-(3-Bromobenzoyl)-11-ethyl-19-methoxy-8,15-diazatetracyclo[9.6.2.0^{2.7.0}8.18]nonadeca-1(18),2,4,6-tetraen-9-one. Compound **74** (18.2 mg, 0.056 mmol) was dissolved in dichloromethane (0.5 mL) before triethylamine (16.0 μL , 0.112 mmol) was added. The mixture was cooled to 0 °C before 3-bromobenzoyl chloride (8.0 μL , 0.061 mmol, 0.3 M in dichloromethane) and 4-dimethylaminopyridine (DMAP, one crystal) were added as a solution in dichloromethane. The reaction was allowed to stir for 3 h as it slowly warmed to room temperature. Upon completion (by TLC), the reaction was quenched with brine, extracted with dichloromethane, and dried with sodium sulfate. The resulting organic layer was then filtered, concentrated in vacuo, and the crude material was purified via column chromatography using a gradient of 100% hexanes to 3:1 hexanes/ethyl acetate to afford **5** (17 mg, 59%) as a white-brown solid. $^1\text{H NMR}$: (400 MHz, CD_3CN at 65 °C) δ 8.38 (dt, J = 8.2, 0.8 Hz, 1H), 7.52–7.44 (m, 3H), 7.39 (td, J = 7.7, 1.1 Hz, 1H), 7.27 (td, J = 7.5, 1.0 Hz, 1H), 7.13 (m, 1H), 7.10 (dd, J = 8.0, 7.8 Hz, 1H), 6.74 (d, J = 8.0 Hz, 1H), 4.54 (s, 1H), 3.64 (m, 1H), 3.52–3.39 (m, 2H), 3.29 (s, 3H), 3.16 (m, 1H), 2.94 (d, J = 17.6 Hz, 1H), 2.71 (dt, J = 14.0, 4.9 Hz, 1H), 2.36 (dd, J = 17.6, 1.3 Hz, 1H), 1.90 (m, 1H), 1.68–1.57 (m, 4H), 0.89 (t, J = 7.6 Hz, 3H), 0.78 (m, 1H). $^{13}\text{C NMR}$: (100 MHz, CD_3CN at 65 °C) δ 172.7, 170.4, 141.1, 136.4, 134.9, 133.0, 131.4, 130.6, 130.4, 126.6, 126.1, 125.0, 123.0, 120.6, 119.5, 117.2, 75.8, 56.8, 51.6, 50.2, 44.4, 41.8, 31.6, 27.3, 23.5, 22.5, 8.2. HRMS (ESI): calcd for $\text{C}_{27}\text{H}_{30}\text{BrN}_4\text{O}_3$ [$\text{M} + \text{Na}$] $^+$: 509.1434, found: 509.1447. MP: 68–70 °C. $[\alpha]_{\text{D}}^{20}$: +52° (c 0.12 g/100 mL, MeOH).



Synthesis Procedure for the Generation of 6, Methyl 2-[(1S,7aR,12bS)-1-Ethyl-7a-hydroxy-1H,2H,3H,4H,6H,7H,7aH,12bH-indolo[2,3-a]quinolizin-1-yl]acetate. Compound **16** (1.18 g, 3.61 mmol) was added to a round-bottom flask and dissolved in anhydrous dichloromethane (132 mL). The resulting solution was cooled to –41 °C (acetonitrile/dry ice), and trifluoroacetic acid (5.0 mL, 61.5 mmol)

was added. The reaction was stirred for 5 min, then *m*-chloroperbenzoic acid (623 mg, 3.61 mmol) was added as a 0.3 M solution in anhydrous dichloromethane (12.0 mL), and the reaction was stirred for 12 h. Then, the reaction was quenched with 3 M aqueous ammonium hydroxide. The neutralized solution was partitioned between dichloromethane and brine, and then the organic layer was dried with sodium sulfate. The organic layer was filtered, concentrated in vacuo, and the crude material was purified via column chromatography using a gradient of 99:1 hexanes/triethylamine to 82.5:16.5:1 hexanes/ethyl acetate/triethylamine to afford **6** (294 mg, 34%) as a white crystalline solid. $^1\text{H NMR}$: (400 MHz, CDCl_3) δ 7.49 (d, J = 7.6 Hz, 1H), 7.41 (d, J = 7.0 Hz, 1H), 7.31 (dd, J = 8.2, 7.7 Hz, 1H), 7.18 (dd, J = 8.2, 7.3 Hz, 1H), 4.48 (m, 1H), 3.55 (s, 3H), 3.12 (s, 1H), 3.06–2.97 (m, 2H), 2.88 (d, J = 13.5 Hz, 1H), 2.62 (ddd, J = 14.4, 9.8, 6.4 Hz, 1H), 2.39 (d, J = 13.5 Hz, 1H), 2.27 (ddd, J = 12.2, 7.8, 6.4 Hz, 1H), 2.10–1.95 (m, 3H), 1.92 (m, 1H), 1.74 (sextet, J = 7.5 Hz, 1H), 1.63 (m, 1H), 1.60–1.42 (m, 2H), 1.05 (t, J = 7.5 Hz, 3H). Note: ^1H spectrum referenced TMS at 0.00 ppm. $^{13}\text{C NMR}$: (100 MHz, CDCl_3) δ 183.8, 173.6, 154.1, 139.9, 129.3, 126.2, 122.3, 121.0, 82.5, 71.5, 55.6, 51.5, 50.8, 40.7, 38.9, 32.2, 31.3, 29.7, 21.4, 8.1. HRMS (ESI): calcd for $\text{C}_{20}\text{H}_{27}\text{N}_2\text{O}_3$ [$\text{M} + \text{H}$] $^+$: 343.2046, found: 343.2036. MP: 122–124 °C. $[\alpha]_{\text{D}}^{20}$: –51° (c 0.12 g/100 mL, MeOH).

General Amidation Procedure for the Synthesis of 7, Methyl (4aS,12bS)-12-[2-[(4-Bromophenyl)formamido]ethyl]-1-cyano-4a-ethyl-1H,2H,3H,4H,4aH,12bH-indolo[1,2-h]1,7-naphthyridine-6-carboxylate. Compound **84** (33.5 mg, 0.089 mmol) was added to a flame-dried round-bottom flask and dissolved in dichloromethane (2.0 mL). The solution was then cooled to 0 °C, before triethylamine (25.0 μL , 0.177 mmol) was added dropwise. 4-Bromobenzoyl chloride (21.4 mg, 0.097 mmol) and 4-dimethylaminopyridine (DMAP, one crystal) in dichloromethane were added dropwise to the reaction. The reaction was allowed to warm to room temperature and proceeded for 5 h. Upon completion (by TLC), the reaction was quenched with saturated aqueous sodium bicarbonate and extracted with dichloromethane. The resulting organic layer was washed with brine, dried with sodium sulfate, filtered, concentrated in vacuo, and finally purified via column chromatography using a gradient of 100% hexanes to 1:1 hexanes/ethyl acetate to yield **7** (33.8 mg, 75%) as a white solid. $^1\text{H NMR}$: (400 MHz, CDCl_3) δ 7.63–7.57 (m, 3H), 7.51–7.46 (m, 2H), 7.24–7.17 (m, 2H), 7.13 (td, J = 7.3, 1.4 Hz, 1H), 6.84 (t, J = 6.2 Hz, 1H), 6.13 (d, J = 1.7 Hz, 1H), 4.04 (d, J = 1.7 Hz, 1H), 3.97 (s, 3H), 3.90–3.75 (m, 2H), 3.35 (ddd, J = 14.6, 7.5, 5.7 Hz, 1H), 3.18 (dt, J = 12.7, 2.1 Hz, 1H), 3.03–2.88 (m, 2H), 2.09 (d, J = 14.1 Hz, 1H), 1.87–1.62 (m, 2H), 1.40 (td, J = 14.1, 4.0 Hz, 1H), 1.11–0.93 (m, 2H), 0.71 (t, J = 7.5 Hz, 3H). $^{13}\text{C NMR}$: (100 MHz, CDCl_3) δ 167.0, 163.4, 134.8, 133.2, 131.7, 130.3, 129.1, 128.9, 127.6, 127.2, 126.2, 124.1, 121.3, 119.6, 118.0, 117.0, 112.7, 56.5, 52.9, 49.4, 41.1, 39.6, 32.3, 31.4, 24.2, 21.9, 8.0. HRMS (ESI): calcd for $\text{C}_{29}\text{H}_{29}\text{BrN}_4\text{O}_3$ [$\text{M} + \text{Na}$] $^+$: 583.1315, found: 583.1299. MP: 83–85 °C. $[\alpha]_{\text{D}}^{20}$: –73° (c 0.10 g/100 mL, MeOH).



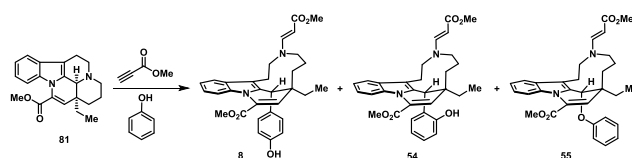
General Procedure for the Synthesis of 8, 54, and 55. Compound **81** (462 mg, 1.37 mmol) was added to a flame-dried round-bottom flask and dissolved in chloroform (137 mL). Then, phenol (5.10 g, 55.0 mmol) was added to the reaction mixture before methyl propiolate (204 μL , 2.06 mmol) was added dropwise. The reaction was heated to 62 °C for 7 h. Upon completion (as monitored by TLC), the reaction was cooled down to room temperature, quenched with saturated aqueous brine, and extracted with dichloromethane. The organic layer was collected and dried with sodium sulfate, filtered,

and concentrated in vacuo. The resulting crude material was then purified via column chromatography using a gradient of 100% hexanes to 3:2 hexanes/ethyl acetate to afford **8** (247 mg, 35%), **54** (96.2 mg, 14%), and **55** (191 mg, 27%) as white solids. Note: this reaction gave various product distributions. For example, this reaction was scaled to 3.4 grams of **81** (10.3 mmol), and, following the same procedure (methyl propiolate: 1.4 mL, 14.4 mmol; phenol: 19.4 g, 206 mmol; chloroform, 206 mL), we isolated 2.5 g of **8** (47% yield), 267 mg of **54** (5%), and 637 mg of **55** (12%).

Analogue **8**, methyl (11*S*,19*S*)-11-ethyl-19-(4-hydroxyphenyl)-15-[(1*E*)-3-methoxy-3-oxoprop-1-en-1-yl]-8,15-diazatetracyclo[9.6.2.0^{2,7}.0^{8,18}]nonadeca-1(18),2,4,6,9-pentaene-9-carboxylate: ¹H NMR: (400 MHz, CDCl₃ at 50 °C) δ 7.67 (d, *J* = 13.3 Hz, 1H), 7.38 (d, *J* = 7.6 Hz, 1H), 7.24–7.09 (m, 3H), 6.93 (d, *J* = 8.3 Hz, 2H), 6.67 (d, *J* = 8.3 Hz, 2H), 6.16 (s, 1H), 5.93 (s, 1H), 4.83 (d, *J* = 13.3 Hz, 1H), 4.11 (s, 1H), 4.00 (s, 3H), 3.77 (s, 3H), 3.74 (m, 1H), 3.52 (dd, *J* = 14.2, 7.1 Hz, 1H), 3.16–2.93 (m, 2H), 2.66 (d, *J* = 13.6 Hz, 1H), 2.53 (dd, *J* = 14.8, 8.3 Hz, 1H), 1.78 (dd, *J* = 14.8, 10.5 Hz, 1H), 1.61 (m, 1H), 1.44–1.17 (m, 2H), 1.08–0.85 (m, 2H), 0.79 (t, *J* = 7.3 Hz, 3H). ¹³C NMR: (100 MHz, CDCl₃ at 50 °C) δ 170.6, 164.6, 155.5, 151.8, 138.0, 135.1, 130.5, 130.3, 130.2, 129.6, 128.7, 122.6, 121.1, 118.0, 115.5, 112.8, 112.2, 86.8, 59.1, 56.4, 52.8, 51.1, 45.6, 43.3, 34.4, 27.2, 21.8 (2), 8.2. Note: characterization of overlapping carbon signals at 21.8 ppm is based on heteronuclear single quantum coherence (HSQC) studies of **58** (related analogue; Supporting Information). HRMS (ESI): calcd for C₃₁H₃₅N₂O₅ [M + H]⁺: 515.2540, found: 515.2547. MP: 157–159 °C. [α]_D²⁰: –134° (c 0.15 g/100 mL, MeOH).

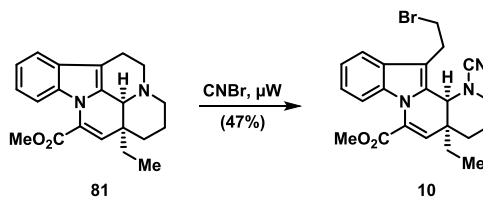
Analogue **54**, methyl (11*S*,19*S*)-11-ethyl-19-(2-hydroxyphenyl)-15-[(1*E*)-3-methoxy-3-oxoprop-1-en-1-yl]-8,15-diazatetracyclo[9.6.2.0^{2,7}.0^{8,18}]nonadeca-1(18),2,4,6,9-pentaene-9-carboxylate: ¹H NMR: (400 MHz, CDCl₃ at 50 °C) δ 7.67 (d, *J* = 13.4 Hz, 1H), 7.38 (d, *J* = 7.3 Hz, 1H), 7.25–7.16 (m, 2H), 7.13 (dd, *J* = 7.2, 1.3 Hz, 1H), 7.02–6.96 (m, 2H), 6.75 (dd, *J* = 7.9, 0.7 Hz, 1H), 6.72 (dd, *J* = 8.2, 7.7 Hz, 1H), 6.29 (m, 1H), 6.25 (s, 1H), 5.11 (s, 1H), 4.76 (d, *J* = 13.4 Hz, 1H), 4.02 (s, 3H), 3.74 (s, 3H), 3.71 (m, 1H), 3.61 (dd, *J* = 14.0, 7.5 Hz, 1H), 3.19 (dd, *J* = 15.2, 13.8 Hz, 1H), 2.98 (dd, *J* = 14.1, 13.0 Hz, 1H), 2.67 (d, *J* = 14.7 Hz, 1H), 2.58 (dd, *J* = 14.3, 8.4 Hz, 1H), 1.93–1.79 (m, 3H), 1.40 (m, 1H), 1.10 (m, 1H), 0.94 (m, 1H), 0.82 (t, *J* = 7.7 Hz, 3H). ¹³C NMR: (125 MHz, CDCl₃ at 50 °C) δ 170.7, 164.7, 154.0, 152.3, 138.2, 135.3, 130.6, 130.0, 129.9 (2), 128.9, 127.6, 126.3, 122.6, 121.0, 118.1, 115.6, 113.4, 112.2, 87.2, 59.5, 57.0, 52.7, 51.0, 44.2, 36.7, 34.7, 24.6, 22.6, 21.7, 8.2. Note: carbon signals at 59.5, 57.0, 22.6, and 21.7 ppm are broad and challenging to observe; however, these can be seen in the HSQC and HSQC–TOCSY spectra (these signals are labeled in each of these corresponding spectra). HRMS (ESI): calcd for C₃₁H₃₅N₂O₅ [M + H]⁺: 515.2540, found: 515.2549. MP: 240–242 °C, decomposed. [α]_D²⁰: –74° (c 0.10 g/100 mL, CH₂Cl₂).

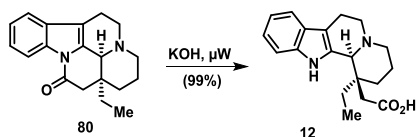
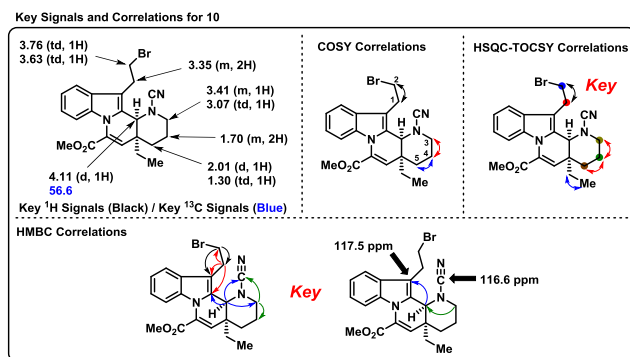
Analogue **55**, methyl (11*S*,19*R*)-11-ethyl-15-[(1*E*)-3-methoxy-3-oxoprop-1-en-1-yl]-19-phenoxy-8,15-diazatetracyclo[9.6.2.0^{2,7}.0^{8,18}]nonadeca-1(18),2,4,6,9-pentaene-9-carboxylate: ¹H NMR: (400 MHz, CDCl₃ at 50 °C) δ 7.59 (d, *J* = 13.4 Hz, 1H), 7.41 (dd, *J* = 7.8, 1.3 Hz, 1H), 7.29 (m, 1H), 7.23 (td, *J* = 6.9, 1.2 Hz, 1H), 7.20–7.12 (m, 3H), 6.96 (m, 1H), 6.88–6.83 (m, 2H), 6.35 (d, *J* = 1.5 Hz, 1H), 5.04 (d, *J* = 1.5 Hz, 1H), 4.78 (d, *J* = 13.4 Hz, 1H), 4.00 (s, 3H), 3.77 (s, 3H), 3.67 (dt, *J* = 13.6, 3.0 Hz, 1H), 3.39 (dd, *J* = 14.4, 8.3 Hz, 1H), 2.87 (dd, *J* = 14.1, 12.6 Hz, 1H), 2.77 (dd, *J* = 15.2, 13.1 Hz, 1H), 2.65 (d, *J* = 14.4 Hz, 1H), 2.48 (ddd, *J* = 14.1, 7.8, 2.4 Hz, 1H), 2.00 (sextet, *J* = 7.5 Hz, 1H), 1.88 (sextet, *J* = 7.5 Hz, 1H), 1.78 (ddd, *J* = 14.1, 7.8, 2.4 Hz, 1H), 1.56 (m, 1H), 1.06 (t, *J* = 7.5 Hz, 3H), 0.99–0.89 (m, 2H). ¹³C NMR: (100 MHz, CDCl₃ at 50 °C) δ 169.6, 164.2, 158.1, 151.3, 135.8, 133.3, 129.8, 129.5, 129.3, 128.0, 123.8, 123.0, 121.0, 119.9, 118.7, 116.0, 112.9, 87.5, 76.0, 59.2, 56.1, 52.6, 50.8, 43.9, 31.8, 26.7, 21.8 (2), 8.2. Note: characterization of overlapping carbon signals at 21.8 ppm is based on HSQC studies of **58** (related analogue; Supporting Information). HRMS (ESI): calcd for C₃₁H₃₄N₂O₅Na [M + Na]⁺: 537.2360, found: 537.2365. MP: 108–110 °C. [α]_D²⁰: +46° (c 0.21 g/100 mL, CH₂Cl₂).



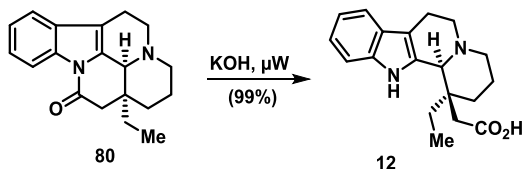
Synthesis Procedure for the Generation of 9, (1*R*,12*S*,19*S*)-12-Ethyl-9,16-diazapentacyclo[10.6.1.0^{1,9}.0^{3,8}.0^{16,19}]nonadeca-3,5,7-triene-2,10-dione. Compound **6** (12.9 mg, 0.038 mmol) was added to a round-bottom flask and dissolved in methanol (1.5 mL). Sodium hydroxide (8.0 mg, 0.19 mmol) was added, and the reaction was heated to 64 °C for 3 h after being equipped with a reflux condenser. Upon completion, the reaction was quenched with brine, extracted with chloroform, and the organic layer was dried with sodium sulfate. The organic layer was filtered, concentrated in vacuo, and the crude material was purified via column chromatography using a gradient of 99:1 hexanes/triethylamine to 74.5:24.5:1 hexanes/ethyl acetate:triethylamine to afford **9** (9.7 mg, 82%) as a white-brown solid. ¹H NMR: (400 MHz, CDCl₃) δ 8.29 (d, *J* = 8.2 Hz, 1H), 7.75 (d, *J* = 7.7 Hz, 1H), 7.66 (td, *J* = 7.8, 1.4 Hz, 1H), 7.24 (m, 1H), 3.44 (d, *J* = 15.6 Hz, 1H), 3.11 (m, 1H), 3.03 (dd, *J* = 8.8, 7.4 Hz, 1H), 2.53 (s, 1H), 2.49 (m, 1H), 2.30 (td, *J* = 11.4, 3.1 Hz, 1H), 2.17 (dd, *J* = 12.4, 5.5 Hz, 1H), 2.11 (dd, *J* = 15.6, 2.1 Hz, 1H), 1.95 (td, *J* = 11.3, 7.8 Hz, 1H), 1.79–1.67 (m, 2H), 1.61 (m, 1H), 1.21 (m, 1H), 0.91 (m, 1H), 0.78–0.69 (m, 4H). ¹³C NMR: (100 MHz, CDCl₃) δ 200.9, 170.9, 152.3, 136.9, 125.0, 124.5, 122.7, 119.9, 75.5, 68.8, 51.6, 51.0, 40.9, 38.4, 38.3, 32.3, 30.1, 22.3, 7.1. HRMS (ESI): calcd for C₁₉H₂₃N₂O₂ [M + H]⁺: 311.1754, found: 311.1756. MP: 115–117 °C. [α]_D²⁰: +363° (c 0.27 g/100 mL, MeOH).

Synthesis Procedure for the Generation of 10, Methyl (4*aS*,12*bS*)-12-(2-Bromoethyl)-1-cyano-4*a*-ethyl-1*H*,2*H*,3*H*,4*H*,4*aH*,12*bH*-indolo[1,2-*h*]1,7-naphthyridine-6-carboxylate. Compound **81** (503 mg, 1.50 mmol) was added to a flame-dried microwave vial and dissolved in *N,N*-dimethylformamide (15 mL). Then, a 3.0 M solution of cyanogen bromide in dichloromethane (1.5 mL, 4.50 mmol) was added dropwise to the reaction, which was subsequently subjected to microwave irradiation for 6 min at 100 °C. Upon completion of the reaction (monitored by TLC), the reaction was cooled down to room temperature, diluted with ethyl acetate, and quenched with brine (3 × 100 mL). The organic layer was collected and dried with sodium sulfate, then filtered, and finally concentrated in vacuo. The crude material was purified via column chromatography using a gradient of 100% chloroform to 99:1 chloroform/acetone to yield **10** (310 mg, 47%) as an orange-white solid. ¹H NMR: (400 MHz, CDCl₃) δ 7.59 (d, *J* = 7.6, 1H), 7.28–7.14 (m, 3H), 6.15 (d, *J* = 1.5 Hz, 1H), 4.11 (d, *J* = 1.5 Hz, 1H), 3.93 (s, 3H), 3.76 (td, *J* = 9.5, 7.1 Hz, 1H), 3.63 (td, *J* = 9.5, 7.1 Hz, 1H), 3.48–3.29 (m, 3H), 3.07 (td, *J* = 12.1, 3.0 Hz, 1H), 2.01 (d, *J* = 13.4 Hz, 1H), 1.79–1.56 (m, 2H), 1.30 (td, *J* = 13.1, 3.9 Hz, 1H), 1.11–0.96 (m, 2H), 0.69 (t, *J* = 7.5 Hz, 3H). Note: ¹H spectrum referenced TMS at 0.00 ppm. ¹³C NMR: (100 MHz, CDCl₃) δ 163.3, 134.6, 130.0, 128.0, 127.9, 127.6, 123.9, 121.2, 119.2, 117.5, 116.6, 112.7, 56.6, 52.8, 49.9, 39.4, 32.2, 31.5, 31.4, 28.6, 21.7, 8.1. HRMS (ESI): calcd for C₂₂H₂₄BrN₃O₂Na [M + Na]⁺: 464.0944, found: 464.0959. MP: 115–117 °C. [α]_D²⁰: –76° (c 0.24 g/100 mL, CH₂Cl₂).





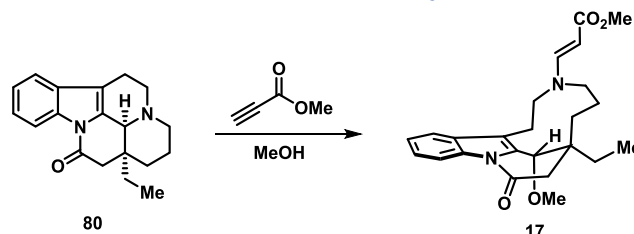
Synthesis Procedure for the Generation of 12, 2-[(1*S*,12*bS*)-1-Ethyl-1*H*,2*H*,3*H*,4*H*,6*H*,7*H*,12*H*,12*bH*-indolo[2,3-*a*]quinolizin-1-yl]-acetic Acid. Lactam **80** (3.53 g, 12.0 mmol) was reacted with potassium hydroxide in seven equal portions in a flame-dried microwave vial. Each portion of **80** was dissolved in ethanol (8.5 mL), and a 5.0 M aqueous potassium hydroxide solution (5 mL) was added. The resulting reaction mixture was then subjected to microwave irradiation for 20 min at 180 °C. The seven individually reacted portions were then combined in an Erlenmeyer flask and acidified to pH 5–6. The resulting solution was then extracted with dichloromethane. The organic layer was collected and then dried with sodium sulfate, filtered, and concentrated in vacuo. The crude material was purified via column chromatography using a 99:1 dichloromethane/triethylamine to a 94:5:1 dichloromethane/methanol/triethylamine solvent system to elute, affording **12** (3.80 g, 99%) as a white solid. ¹H NMR: (400 MHz, DMSO-*d*₆) δ 12.59 (s, 1H), 9.86 (s, 1H), 7.46 (d, *J* = 8.1 Hz, 1H), 7.36 (d, *J* = 7.5 Hz, 1H), 7.03 (dd, *J* = 8.7, 7.5 Hz, 1H), 6.95 (dd, *J* = 8.4, 7.4 Hz, 1H), 3.40 (s, 1H), 3.02–2.97 (m, 2H), 2.81–2.72 (m, 2H), 2.60–2.48 (m, 2H), 2.40 (td, *J* = 11.7, 2.7 Hz, 1H), 2.04 (sextet, *J* = 7.5 Hz, 1H), 1.95–1.82 (m, 2H), 1.77 (sextet, *J* = 7.5 Hz, 1H), 1.66 (d, *J* = 14.2 Hz, 1H), 1.59–1.48 (m, 2H), 1.06 (t, *J* = 7.5 Hz, 3H). Note: TMS was referenced at 0.00 ppm for this spectrum. ¹³C NMR: (100 MHz, DMSO-*d*₆) δ 174.1, 136.6, 132.1, 126.1, 120.8, 118.5, 117.2, 111.8, 110.6, 66.1, 56.0, 53.2, 39.2, 38.9, 31.4, 31.1, 21.7, 21.5, 8.4. HRMS (ESI): calcd for C₁₉H₂₅N₂O₂ [*M* + *H*]⁺: 313.1911, found: 313.1918. MP: 204–206 °C, lit. 203–206 °C.²¹ [*α*]_D²⁰: –207° (c 0.13 g/100 mL, CH₂Cl₂).



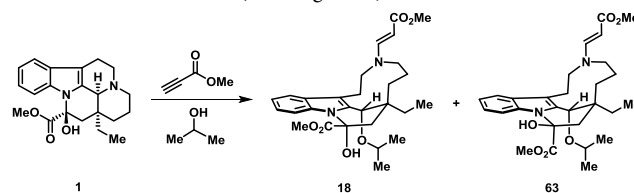
Synthesis Procedure for the Generation of 16, Methyl 2-[(1*S*,12*bS*)-1-Ethyl-1*H*,2*H*,3*H*,4*H*,6*H*,7*H*,12*H*,12*bH*-indolo[2,3-*a*]quinolizin-1-yl]acetate. Compound **12** (1.51 g, 4.84 mmol) was added to a round-bottom flask and dissolved in anhydrous *N,N*-dimethylformamide (48 mL). The solution was cooled to 0 °C, and then anhydrous potassium carbonate (1.34 g, 9.69 mmol) and iodomethane (0.362 mL, 5.81 mmol) were added sequentially. The resulting reaction mixture was warmed slowly to room temperature and reacted for 3 h. Upon completion by TLC, the reaction was quenched with brine, extracted with ethyl acetate, and the organic layer was washed with deionized water three times (~1 L). The organic layer was dried with sodium sulfate, filtered, concentrated in vacuo, and the crude material was purified via column chromatography using a gradient of 99:1 hexanes/triethylamine to 82.5:16.5:1 hexanes/ethyl acetate:triethylamine to afford **16** (1.18 g, 75%) as a brown solid. ¹H NMR: (400 MHz, CDCl₃) δ 7.83 (s, 1H), 7.47 (d, *J* = 7.8 Hz, 1H), 7.32 (d, *J* = 8.0 Hz, 1H), 7.15 (td, *J* = 8.0, 1.3 Hz, 1H),

7.09 (td, *J* = 8.0, 1.1 Hz, 1H), 3.49 (s, 3H), 3.38 (m, 1H), 3.09–2.97 (m, 3H), 2.89 (m, 1H), 2.68–2.53 (m, 2H), 2.40 (td, *J* = 12.5, 2.8 Hz, 1H), 2.06–1.86 (m, 3H), 1.82 (m, 1H), 1.67–1.55 (m, 3H), 1.18 (t, *J* = 7.7 Hz, 3H). ¹³C NMR: (100 MHz, CDCl₃) δ 173.7, 136.1, 132.6, 126.8, 121.7, 119.4, 117.9, 112.4, 110.9, 66.3, 56.9, 54.0, 51.2, 40.4, 38.1, 32.3, 31.4, 22.2, 22.1, 8.2. HRMS (ESI): calcd for C₂₀H₂₇N₂O₂ [*M* + *H*]⁺: 327.2067, found: 327.2074. MP: 127–129 °C. [*α*]_D²⁰: –52° (c 0.74 g/100 mL, CH₂Cl₂).

Synthesis Procedure for the Generation of 17, Methyl (2*E*)-3-[(1*S*,19*R*)-11-Ethyl-19-methoxy-9-oxo-8,15-diazatetracyclo[9.6.2.0^{2,7}.0^{8,18}]nonadeca-1(18),2,4,6-tetraen-15-yl]prop-2-enoate. Lactam **80** (38.9 mg, 0.132 mmol) was added to a round-bottom flask and dissolved in methanol (13 mL). Methyl propiolate (18 μL, 0.198 mmol) was then added dropwise, and the reaction was stirred at room temperature for 5 min before heating to reflux for 22 h. Upon completion (by TLC), the reaction was quenched with saturated aqueous brine and extracted with ethyl acetate. The organic layer was collected, dried with sodium sulfate, filtered, and concentrated in vacuo. The crude material was purified via column chromatography using a gradient of 100% hexanes to 2:1 hexanes/ethyl acetate to afford **17** (44.9 mg, 83%) as a white solid. ¹H NMR: (400 MHz, CDCl₃ at 50 °C) δ 8.46 (d, *J* = 7.4 Hz, 1H), 7.55 (d, *J* = 13.3 Hz, 1H), 7.48 (dd, *J* = 7.4, 0.7 Hz, 1H), 7.39 (td, *J* = 7.4, 0.7 Hz, 1H), 7.32 (td, *J* = 7.4, 0.7 Hz, 1H), 4.80 (d, *J* = 13.4 Hz, 1H), 4.14 (s, 1H), 3.72 (m, 1H), 3.71 (s, 3H), 3.55 (dd, *J* = 14.2, 6.8 Hz, 1H), 3.21 (s, 3H), 3.14 (td, *J* = 14.1, 2.6 Hz, 1H), 3.01 (d, *J* = 17.3 Hz, 1H), 2.93 (m, 1H), 2.38 (d, *J* = 17.4 Hz, 1H), 2.33 (m, 1H), 1.94 (sextet, *J* = 7.6 Hz, 1H), 1.88–1.69 (m, 3H), 1.62–1.52 (m, 2H), 0.87 (t, *J* = 7.7 Hz, 3H), 0.84 (m, 1H). ¹³C NMR: (100 MHz, CDCl₃ at 50 °C) δ 169.6, 169.4, 150.4, 135.5, 133.7, 128.9, 126.0, 124.1, 118.9, 118.2, 117.2, 87.9, 75.5, 58.9, 56.5, 55.8, 50.9, 43.6, 40.9, 34.1, 26.6, 22.4, 22.0, 7.9. HRMS (ESI): calcd for C₂₄H₃₁N₂O₄ [*M* + *H*]⁺: 411.2278, found: 411.2269. MP: 116–118 °C. [*α*]_D²⁰: +37° (c 0.15 g/100 mL, CH₂Cl₂). Note: X-ray data of **17** can be found in the Supporting Information.



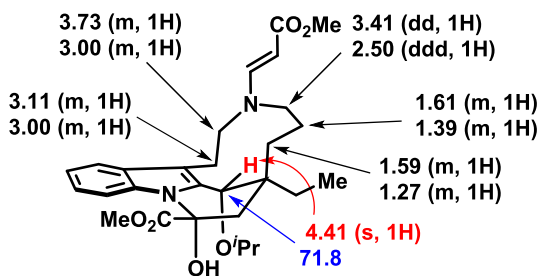
Synthesis Procedure for the Generation of 18 and 63. Vincamine **1** (100 mg, 0.282 mmol) was added to a flame-dried round-bottom flask and dissolved in isopropanol (28 mL). Methyl propiolate (41 μL, 0.462 mmol) was then added dropwise to the mixture, and the reaction was heated to reflux for 2 h. Upon completion, the reaction was cooled and then concentrated in vacuo. Finally, the crude material was purified via column chromatography using a gradient of 100% hexanes to 3:1 hexanes/ethyl acetate to afford **18** (84.4 mg, 60%) as a colorless solid and **V3m** (35.7 mg, 25%) as a clear-brown residue.



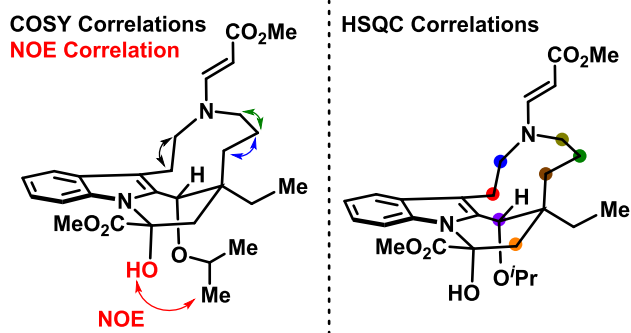
Analogue **18**, methyl (9*R*,11*S*,19*R*)-11-ethyl-9-hydroxy-15-[(1*E*)-3-methoxy-3-oxoprop-1-en-1-yl]-19-(propan-2-yloxy)-8,15-diazatetracyclo[9.6.2.0^{2,7}.0^{8,18}]nonadeca-1(18),2,4,6-tetraene-9-carboxylate: ¹H NMR: (400 MHz, CDCl₃ at 50 °C) δ 7.56–7.50 (m, 2H), 7.20–7.11 (m, 2H), 7.08 (m, 1H), 4.95 (s, 1H), 4.75 (d, *J* = 13.3 Hz, 1H), 4.41 (s, 1H), 3.83 (s, 3H), 3.73 (m, 1H), 3.67 (s, 3H), 3.51 (septet, *J* = 5.9 Hz, 1H), 3.41 (dd, *J* = 14.0, 8.1 Hz, 1H), 3.11 (m, 1H), 3.04–2.94 (m, 2H), 2.50 (ddd, *J* = 14.1, 8.1, 2.0 Hz, 1H), 2.44 (d, *J* = 14.7 Hz, 1H), 2.27 (d, *J* = 14.6 Hz, 1H), 1.87 (sextet, *J* = 7.5 Hz, 1H), 1.70–1.53 (m, 3H), 1.39 (m, 1H), 1.27 (m, 1H), 1.15 (d, *J* = 5.9 Hz,

3H), 0.92 (d, $J = 5.9$ Hz, 3H), 0.86 (t, $J = 7.5$ Hz, 3H). ^{13}C NMR: (100 MHz, CDCl_3 at 50 °C) δ 172.0, 169.6, 151.3, 135.4, 134.6, 127.6, 123.0, 120.3, 118.5, 111.9, 111.0, 86.7, 82.3, 71.8, 68.9, 58.0, 56.1, 53.4, 50.6, 46.5, 41.8, 34.1, 29.4, 23.4, 22.3 (2), 21.2, 8.1. Note: the presence of two carbon signals at 22.3 ppm was elucidated by a HSQC experiment. HRMS (ESI): calcd for $\text{C}_{28}\text{H}_{38}\text{N}_2\text{O}_6\text{Na}$ [$\text{M} + \text{Na}$] $^+$: 521.2622, found: 521.2628. MP: 158–160 °C. $[\alpha]_{\text{D}}^{20}$: +62° (c 0.27 g/100 mL, CH_2Cl_2).

Key Signals and Correlations for 18

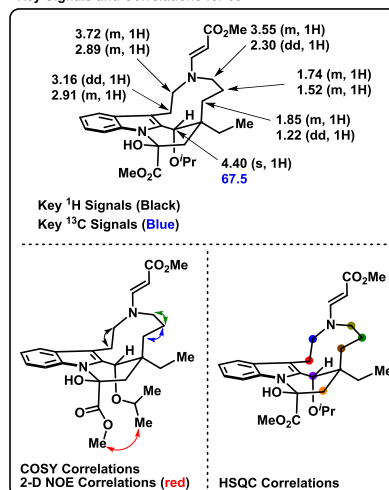


Key ^1H Signals (Black or Red), Key ^{13}C Signals (Blue)

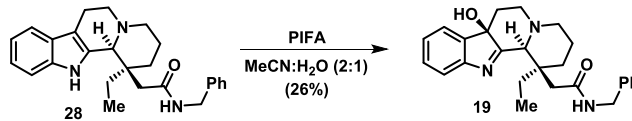


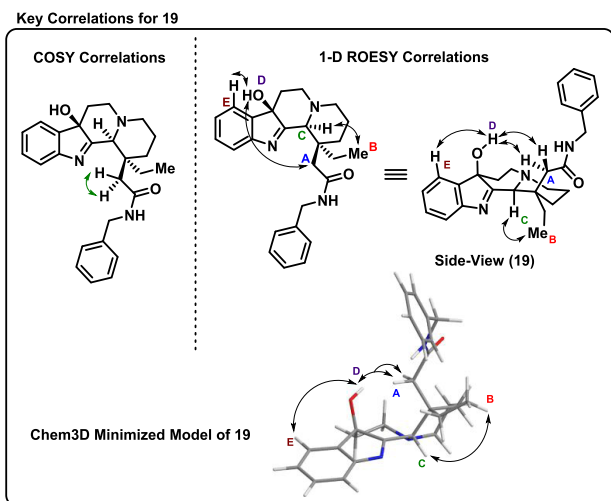
Analogue 63, methyl (9S,11S,19R)-11-ethyl-9-hydroxy-15-[(1E)-3-methoxy-3-oxoprop-1-en-1-yl]-19-(propan-2-yloxy)-8,15-diazatetracyclo[9.6.2.0^{2,7}.0^{8,18}]nonadeca-1(18),2,4,6-tetraene-9-carboxylate: ^1H NMR: (400 MHz, CDCl_3 at 50 °C) δ 7.61 (d, $J = 13.3$ Hz, 1H), 7.51 (m, 1H), 7.22–7.12 (m, 3H), 4.82 (d, $J = 13.3$ Hz, 1H), 4.55 (s, 1H), 4.40 (s, 1H), 3.80 (s, 3H), 3.72 (m, 1H), 3.71 (s, 3H), 3.59–3.47 (m, 2H), 3.16 (dd, $J = 15.7, 13.8$ Hz, 1H), 3.00–2.81 (m, 2H), 2.85 (d, $J = 13.7$ Hz, 1H), 2.30 (dd, $J = 13.8, 9.2$ Hz, 1H), 1.93–1.70 (m, 4H), 1.60–1.49 (m, 2H), 1.22 (dd, $J = 15.9, 7.9$ Hz, 1H), 1.14 (d, $J = 6.0$ Hz, 3H), 0.90 (d, $J = 6.1$ Hz, 3H), 0.86 (t, $J = 7.6$ Hz, 3H). ^{13}C NMR: (100 MHz, CDCl_3 at 50 °C) δ 175.0, 169.7, 150.6, 135.6, 135.2, 128.3, 122.9, 120.5, 118.5, 112.6, 112.3, 87.3, 83.2, 70.3, 67.5, 59.4, 56.7, 54.0, 50.7, 41.0, 40.9, 33.2, 27.3, 23.7, 22.0 (2), 21.3, 8.1. Note: justification for the overlapping carbon signals at 22.0 ppm is based on HSQC studies of 18. HRMS (ESI): calcd for $\text{C}_{28}\text{H}_{38}\text{N}_2\text{O}_6\text{Na}$ [$\text{M} + \text{Na}$] $^+$: 521.2622, found: 521.2630. $[\alpha]_{\text{D}}^{20}$: +58° (c 0.10 g/100 mL, CH_2Cl_2).

Key Signals and Correlations for 63

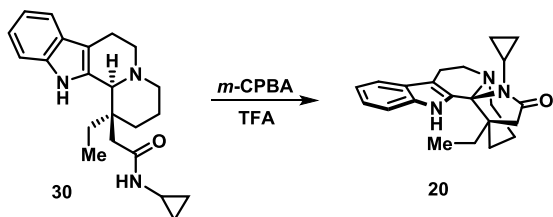


Synthesis Procedure for the Generation of 19, 2-[(15,7aR,12bS)-1-Ethyl-7a-hydroxy-1H,2H,3H,4H,6H,7H,7aH,12bH-indolo[2,3-a]quinolizin-1-yl]-N-benzylacetamide. Compound 28 (403 mg, 1.00 mmol) was added to a round-bottom flask and dissolved in acetonitrile/water (2:1, 30 mL). The resulting solution was cooled to 0 °C, and a 0.3 M solution of [bis(trifluoroacetoxy)iodo]benzene (PIFA; 860 mg, 2.00 mmol) in acetonitrile was added slowly via syringe over 5 min. The reaction was stirred for 3 h at 0 °C and then quenched with cold saturated aqueous sodium bicarbonate. The mixture was then extracted with dichloromethane, washed with brine, and the organic layer was dried with sodium sulfate. The organic layer was filtered, concentrated in vacuo, and the crude material was purified via column chromatography using a gradient of 99:1 hexanes/triethylamine to 49.5:49.5:1 hexanes/ethyl acetate/triethylamine to afford 19 (109 mg, 26%) as a brown residue. ^1H NMR: (500 MHz, CDCl_3) δ 7.49 (d, $J = 7.5$ Hz, 1H), 7.41 (d, $J = 7.2$ Hz, 1H), 7.32 (dd, $J = 8.2, 7.7$ Hz, 1H), 7.29–7.16 (m, 4H), 7.12 (d, $J = 7.4$ Hz, 2H), 6.09 (t, $J = 5.3$ Hz, 1H), 4.36 (dd, $J = 14.6, 5.9$ Hz, 1H), 3.87 (dd, $J = 14.4, 5.0$ Hz, 1H), 3.12 (s, 1H), 3.08–2.99 (m, 2H), 2.65 (m, 1H), 2.60 (d, $J = 14.5$ Hz, 1H), 2.40 (d, $J = 13.6$ Hz, 1H), 2.30 (ddd, $J = 12.2, 7.1, 1.8$ Hz, 1H), 2.13–1.82 (m, 5H), 1.65 (m, 1H), 1.54 (ddd, $J = 13.9, 9.9, 3.3$ Hz, 1H), 1.47 (td, $J = 13.1, 3.9$ Hz, 1H), 1.09 (t, $J = 7.4$ Hz, 3H). ^{13}C NMR: (100 MHz, CDCl_3) δ 184.1, 171.9, 154.1, 139.9, 138.3, 129.3, 128.7, 128.0, 127.4, 126.2, 122.3, 121.0, 82.6, 72.0, 55.7, 50.9, 43.6, 41.0, 40.8, 32.9, 32.2, 29.9, 21.4, 8.3. HRMS (ESI): calcd for $\text{C}_{26}\text{H}_{32}\text{N}_3\text{O}_2$ [$\text{M} + \text{H}$] $^+$: 418.2489, found: 418.2484. $[\alpha]_{\text{D}}^{20}$: +16° (c 0.37 g/100 mL, CH_2Cl_2). Note: correlated spectroscopy (COSY) and 1-D rotating frame overhauser enhancement spectroscopy (ROESY) were used to determine the relative stereochemistry of 19 (see the Supporting Information).





General Procedure for the Oxidative Ring Fusion Synthesis of 20–25 and 46–52 from Corresponding Amide Precursors (e.g., 30). Amide 30 (44.6 mg, 0.127 mmol) was added to a flame-dried round-bottom flask and dissolved in anhydrous dichloromethane (5.1 mL). The reaction was cooled to 0 °C, and trifluoroacetic acid (0.175 mL, 2.16 mmol) was added. The resultant solution was stirred for 5 min, and then *m*-chloroperoxybenzoic acid (21.9 mg, 0.127 mmol) was added as a 0.3 M solution in anhydrous dichloromethane. The reaction was then refluxed for 24 h. Upon completion, the reaction was quenched with 3 M aqueous ammonium hydroxide. The resulting mixture was then extracted with dichloromethane, washed with brine, and the organic layer was dried with sodium sulfate. The organic layer was filtered, concentrated in vacuo, and the crude material was purified via column chromatography using a gradient of 99:1 hexanes/triethylamine to 79.5:19.5:1 hexanes/ethyl acetate/triethylamine to afford ring fusion product 20 (18.5 mg, 42%) as a green-yellow residue.



Analogue 20, (1*S*,17*S*)-20-cyclopropyl-17-ethyl-3,13,20-triazapentacyclo[11.7.0.0^{1,17}.0^{2,10}.0^{4,9}]icosa-2(10),4,6,8-tetraen-19-one. Yield: 42%; 18.5 mg 20; green-yellow residue. ¹H NMR: (400 MHz, CDCl₃) δ 9.47 (s, 1H), 7.55 (d, *J* = 8.2 Hz, 1H), 7.51 (d, *J* = 7.8 Hz, 1H), 7.17 (td, *J* = 7.4, 1.0 Hz, 1H), 7.09 (dd, *J* = 8.2, 7.5 Hz, 1H), 3.53 (ddd, *J* = 11.6, 9.1, 4.5 Hz, 1H), 3.21–3.10 (m, 2H), 3.04 (m, 1H), 3.03 (d, *J* = 16.7 Hz, 1H), 2.89–2.72 (m, 2H), 2.17 (d, *J* = 17.1 Hz, 1H), 2.14 (m, 1H), 1.94 (m, 1H), 1.81 (m, 1H), 1.59–1.35 (m, 3H), 1.13 (sextet, *J* = 7.5 Hz, 1H), 0.80 (m, 1H; buried under triplet), 0.78 (t, *J* = 7.5 Hz, 3H), 0.55 (m, 1H), 0.39–0.22 (m, 2H). ¹³C NMR: (100 MHz, CDCl₃) δ 175.5, 136.9, 133.3, 126.2, 122.1, 119.2, 118.3, 113.5, 112.2, 84.6, 50.4, 49.9, 44.5, 43.7, 33.1, 26.7, 24.7, 22.6, 20.0, 9.4, 6.8, 5.4. HRMS (ESI): calcd for C₂₂H₂₈N₃O [M + H]⁺: 350.2227, found: 350.2213. [α]_D²⁰: +92° (c 0.22 g/100 mL, CH₂Cl₂).

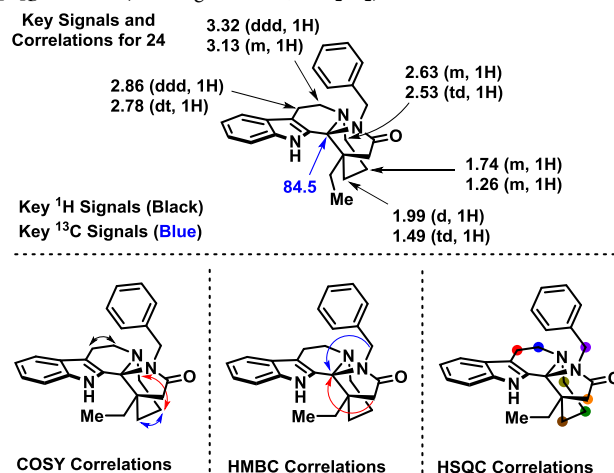
Analogue 21, (1*S*,17*S*)-17-ethyl-20-(prop-2-yn-1-yl)-3,13,20-triazapentacyclo[11.7.0.0^{1,17}.0^{2,10}.0^{4,9}]icosa-2(10),4,6,8-tetraen-19-one. Yield: 56%; 27.5 mg 21; off-white residue. ¹H NMR: (400 MHz, CDCl₃) δ 9.63 (s, 1H), 7.66 (dt, *J* = 8.1, 0.8 Hz, 1H), 7.53 (d, *J* = 7.9 Hz, 1H), 7.20 (ddd, *J* = 7.9, 6.9, 1.2 Hz, 1H), 7.11 (ddd, *J* = 8.1, 6.9, 0.8 Hz, 1H), 3.94 (dd, *J* = 17.3, 2.6 Hz, 1H), 3.61 (dd, *J* = 17.3, 2.6 Hz, 1H), 3.47–3.34 (m, 2H), 3.25 (m, 1H), 3.16 (d, *J* = 17.0 Hz, 1H), 3.01 (dt, *J* = 12.8, 4.2 Hz, 1H), 2.94–2.79 (m, 2H), 2.31 (d, *J* = 17.0 Hz, 1H), 2.05 (m, 1H), 1.98 (t, *J* = 2.6 Hz, 1H), 1.88 (m, 1H), 1.68–1.52 (m, 2H), 1.47 (m, 1H), 1.33 (sextet, *J* = 7.6 Hz, 1H), 0.86 (t, *J* = 7.6 Hz, 3H). ¹³C NMR: (100 MHz, CDCl₃) δ 174.4, 137.5, 131.6,

126.0, 122.4, 119.2, 118.2, 114.4, 112.4, 83.6, 78.9, 70.8, 50.1, 49.6, 43.9, 43.7, 32.8, 29.8, 27.1, 22.2, 18.0, 9.5. HRMS (ESI): calcd for C₂₂H₂₆N₃O [M + H]⁺: 348.2070, found: 348.2075. [α]_D²⁰: +22° (c 0.23 g/100 mL, CH₂Cl₂).

Analogue 22, (1*S*,17*S*)-20-butyl-17-ethyl-3,13,20-triazapentacyclo[11.7.0.0^{1,17}.0^{2,10}.0^{4,9}]icosa-2(10),4,6,8-tetraen-19-one. Yield: 43%; 27.0 mg 22; light green solid. ¹H NMR: (400 MHz, CDCl₃) δ 9.41 (s, 1H), 7.54–7.47 (m, 2H), 7.16 (td, *J* = 8.2, 1.1 Hz, 1H), 7.08 (td, *J* = 7.9, 0.9 Hz, 1H), 3.39 (m, 1H), 3.25–3.10 (m, 2H), 3.10–2.91 (m, 4H), 2.88–2.74 (m, 2H), 2.19 (d, *J* = 16.8 Hz, 1H), 2.02 (m, 1H), 1.82 (m, 1H), 1.62–1.45 (m, 2H), 1.45–1.11 (m, 4H), 1.06–0.92 (m, 2H), 0.80 (t, *J* = 7.5 Hz, 3H), 0.59 (t, *J* = 7.3 Hz, 3H). ¹³C NMR: (100 MHz, CDCl₃) δ 174.6, 137.3, 133.1, 126.2, 122.2, 119.2, 118.2, 113.5, 112.1, 83.5, 50.3, 50.0, 44.4, 43.7, 41.3, 32.8, 30.0, 26.6, 22.4, 20.7, 18.3, 13.7, 9.6. HRMS (ESI): calcd for C₂₃H₃₂N₃O [M + H]⁺: 366.2540, found: 366.2547. MP: 170–172 °C. [α]_D²⁰: +48° (c 0.17 g/100 mL, CH₂Cl₂).

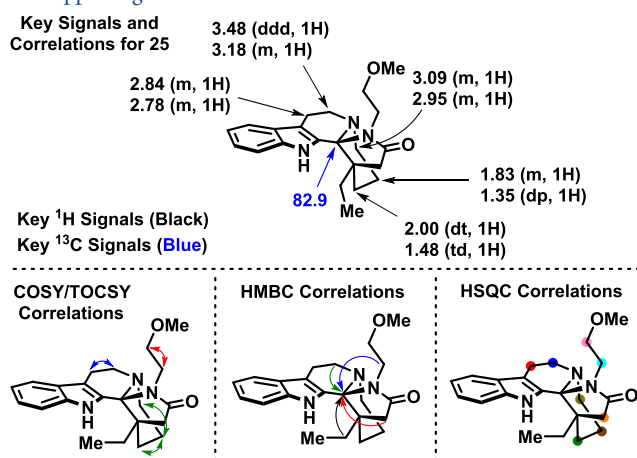
Analogue 23, (1*S*,17*S*)-20-cyclopentyl-17-ethyl-3,13,20-triazapentacyclo[11.7.0.0^{1,17}.0^{2,10}.0^{4,9}]icosa-2(10),4,6,8-tetraen-19-one. Yield: 37%; 24.0 mg 23; off-white solid. ¹H NMR: (400 MHz, CDCl₃) δ 9.18 (s, 1H), 7.50 (d, *J* = 7.8 Hz, 1H), 7.45 (d, *J* = 8.1 Hz, 1H), 7.17 (dd, *J* = 8.3, 7.2 Hz, 1H), 7.08 (dd, *J* = 8.1, 7.3 Hz, 1H), 3.66 (p, *J* = 8.9, 1H), 3.58 (ddd, *J* = 11.7, 8.1, 2.2 Hz, 1H), 3.25–3.12 (m, 2H), 3.00–2.86 (m, 2H), 2.94 (d, *J* = 16.7 Hz, 1H), 2.78 (dt, *J* = 15.2, 4.2 Hz, 1H), 2.46 (m, 1H), 2.09 (d, *J* = 16.5 Hz, 1H), 2.01 (d, *J* = 13.8, 1H), 1.90–1.71 (m, 4H), 1.66–1.44 (m, 3H), 1.43–1.29 (m, 2H), 1.23–1.04 (m, 2H), 0.82 (m, 1H), 0.79 (t, *J* = 7.4 Hz, 3H). ¹³C NMR: (125 MHz, CDCl₃) δ 173.4, 137.2, 133.3, 126.3, 122.3, 119.3, 118.3, 113.5, 111.9, 83.6, 52.9, 50.0, 49.8, 45.3, 43.3, 32.4, 28.7, 28.0, 26.8, 25.3, 24.8, 22.2, 17.1, 9.7. HRMS (ESI): calcd for C₂₄H₃₂N₃O [M + H]⁺: 378.2540, found: 378.2546. MP: 210–212 °C. [α]_D²⁰: +22° (c 0.20 g/100 mL, CH₂Cl₂).

Analogue 24, (1*S*,17*S*)-20-benzyl-17-ethyl-3,13,20-triazapentacyclo[11.7.0.0^{1,17}.0^{2,10}.0^{4,9}]icosa-2(10),4,6,8-tetraen-19-one. Yield: 44%; 20.0 mg 24; light green solid. ¹H NMR: (400 MHz, CDCl₃) δ 8.52 (s, 1H), 7.46 (m, 1H), 7.21–7.17 (m, 3H), 7.15–6.98 (m, 5H), 4.43 (d, *J* = 14.6 Hz, 1H), 3.87 (d, *J* = 14.7 Hz, 1H), 3.32 (ddd, *J* = 11.6, 6.5, 5.1 Hz, 1H), 3.13 (m, 1H), 2.92 (d, *J* = 17.0 Hz, 1H), 2.86 (ddd, *J* = 14.8, 7.9, 5.5 Hz, 1H), 2.78 (dt, *J* = 15.2, 4.6 Hz, 1H), 2.63 (m, 1H), 2.53 (ddd, *J* = 13.3, 10.2, 3.2 Hz, 1H), 2.31 (d, *J* = 16.9 Hz, 1H), 1.99 (m, 1H), 1.72 (m, 1H), 1.57 (sextet, *J* = 7.2 Hz, 1H), 1.49 (m, 1H), 1.33–1.15 (m, 2H), 0.81 (t, *J* = 7.2 Hz, 3H). ¹³C NMR: (100 MHz, CDCl₃) δ 175.2, 137.8, 137.4, 132.5, 128.7, 128.1, 126.8, 126.0, 122.3, 119.1, 118.2, 114.3, 112.1, 84.5, 49.9, 49.6, 44.8, 44.3, 43.6, 32.8, 27.2, 22.3, 17.7, 9.6. HRMS (ESI): calcd for C₂₆H₃₀N₃O [M + H]⁺: 400.2383, found: 400.2393. MP: 90–92 °C. [α]_D²⁰: +24° (c 0.20 g/100 mL, CH₂Cl₂).



Analogue 25, (1*S*,17*S*)-17-ethyl-20-(2-methoxyethyl)-3,13,20-triazapentacyclo[11.7.0.0^{1,17}.0^{2,10}.0^{4,9}]icosa-2(10),4,6,8-tetraen-19-one. Yield: 41%; 18.5 mg 25; white solid. ¹H NMR: (500 MHz, CDCl₃) δ 8.60 (s, 1H), 7.49 (d, *J* = 7.8 Hz, 1H), 7.42 (d, *J* = 8.0 Hz, 1H), 7.18 (ddd, *J* = 8.2, 7.0, 1.2 Hz, 1H), 7.09 (dd, *J* = 8.1, 7.5 Hz,

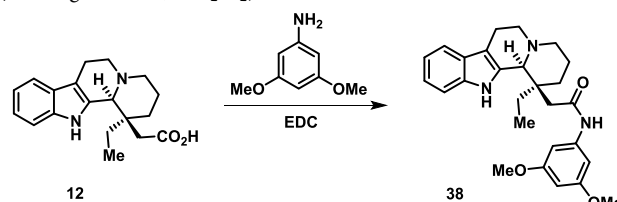
1H), 3.54 (dt, $J = 13.9, 7.1$ Hz, 1H), 3.48 (ddd, $J = 11.8, 7.2, 4.9$ Hz, 1H), 3.21–3.03 (m, 5H), 2.97 (s, 3H), 2.95 (m, 1H), 2.89–2.75 (m, 2H), 2.87 (d, $J = 16.8$ Hz, 1H), 2.19 (d, $J = 16.7$ Hz, 1H), 2.00 (dt, $J = 14.0, 3.7$ Hz, 1H), 1.83 (m, 1H), 1.57 (sextet, $J = 7.4$ Hz, 1H), 1.48 (td, $J = 13.4, 3.7$ Hz, 1H), 1.35 (dp, $J = 13.3, 4.2$ Hz, 1H), 1.17 (sextet, $J = 7.4$ Hz, 1H), 0.78 (t, $J = 7.4$ Hz, 3H). ^{13}C NMR: (150 MHz, CDCl_3) δ 174.6, 137.5, 133.6, 126.6, 122.7, 119.6, 118.5, 113.9, 112.0, 82.9, 69.4, 58.6, 49.9, 44.4, 43.8, 39.9, 32.4, 26.7, 22.2, 17.6, 9.6. HRMS (ESI): calcd for $\text{C}_{22}\text{H}_{30}\text{N}_3\text{O}_2$ [$\text{M} + \text{H}$] $^+$: 368.2333, found: 368.2343. MP: 194–196 °C, decomposed. $[\alpha]_{\text{D}}^{20}$: +61° (c 0.20 g/100 mL, CH_2Cl_2). X-ray: structure and supporting data can be viewed in the Supporting Information.



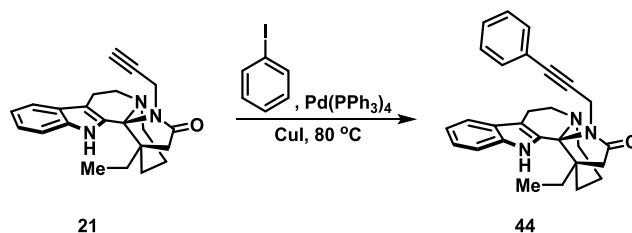
Synthesis Procedure for the Generation of 24 from 19. Compound 19 (26.0 mg, 0.062 mmol) was added to a flame-dried round-bottom flask and dissolved in anhydrous dichloromethane (2.5 mL). The reaction was cooled to 0 °C, and trifluoroacetic acid (0.085 mL, 1.05 mmol) was added. The reaction was slowly warmed to reflux and allowed to react for 2 h. Upon completion, the reaction was quenched with 3 M aqueous ammonium hydroxide. The resulting mixture was then extracted with dichloromethane, washed with brine, and the organic layer was dried with sodium sulfate, filtered, and concentrated in vacuo. The crude product was then purified via column chromatography using a gradient of 99:1 hexanes/triethylamine to afford 24 (18.3 mg, 74%) as a light green solid. Note: this experiment was critical to understanding the reaction mechanism for the oxidative ring fusion to related structures.

Procedure for the Synthesis of 38, 2-[(1S,12bS)-1-Ethyl-1H,2H,3H,4H,6H,7H,12H,12bH-indolo[2,3-a]quinolizin-1-yl]-N-(3,5-dimethoxyphenyl)acetamide. 12 (32.8 mg, 0.105 mmol) was added to a flame-dried round-bottom flask and dissolved in anhydrous dichloromethane (2.6 mL). 1-Ethyl-3-(3-dimethylaminopropyl)-carbodiimide (24.0 μL , 0.136 mmol) was added dropwise, and the reaction was stirred for 5 min. Over a period of 20 min, 3,5-dimethoxyaniline (21.0 mg, 0.136 mmol) as a 0.3 M solution in anhydrous dichloromethane was added, and the reaction proceeded for 72 h. Upon completion, the reaction was quenched with deionized water, extracted with ethyl acetate, and the organic layer was dried with sodium sulfate. The organic layer was then filtered, concentrated in vacuo, and the crude material was purified via column chromatography using a gradient of 99:1 hexanes/triethylamine to 74.5:24.5:1 hexanes/ethyl acetate/triethylamine to afford 38 (10.1 mg, 21%) as a white-brown residue. ^1H NMR: (500 MHz, CDCl_3) δ 8.14 (s, 1H), 7.89 (s, 1H), 7.41 (d, $J = 7.8$ Hz, 1H), 7.30 (d, $J = 8.1$ Hz, 1H), 7.13 (dd, $J = 8.0, 7.5$ Hz, 1H), 7.06 (dd, $J = 8.3, 7.5$ Hz, 1H), 6.50 (d, $J = 2.2$ Hz, 2H), 6.12 (t, $J = 2.2$ Hz, 1H), 3.69 (s, 6H), 3.45 (s, 1H), 3.15–3.05 (m, 2H), 2.98 (m, 1H), 2.76–2.67 (m, 2H), 2.64 (td, $J = 11.4, 3.5$ Hz, 1H), 2.47 (td, $J = 12.8, 2.3$ Hz, 1H), 2.27 (d, $J = 14.3$ Hz, 1H), 2.10–1.93 (m, 4H), 1.70–1.58 (m, 2H), 1.20 (t, $J = 7.6$ Hz, 3H). ^{13}C NMR: (100 MHz, CDCl_3) δ 171.0, 161.0, 140.1, 136.3, 132.7, 126.9, 122.1, 119.8, 118.1, 112.3, 111.1, 97.6, 96.5, 67.2, 56.9, 55.5, 54.2, 43.1, 41.0, 33.2, 32.6, 22.3, 22.2, 8.4. HRMS (ESI): calcd

for $\text{C}_{27}\text{H}_{34}\text{N}_3\text{O}_3$ [$\text{M} + \text{H}$] $^+$: 448.2595, found: 448.2595. $[\alpha]_{\text{D}}^{20}$: –40° (c 0.10 g/100 mL, CH_2Cl_2).

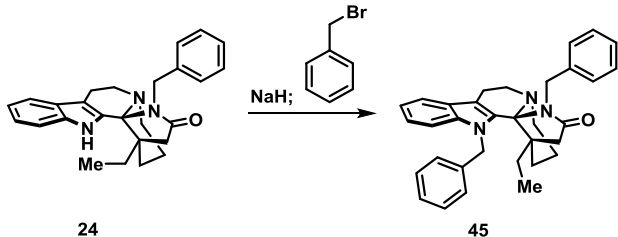


Procedure for the Chemical Synthesis of 44, (1S,17S)-17-Ethyl-20-(3-phenylprop-2-yn-1-yl)-3,13,20-triazapentacyclo[11.7.0.0 1,17 .0 2,10 .0 4,9]jicosa-2(10),4,6,8-tetraen-19-one. To a flame-dried round-bottom flask was added tetrakis(triphenylphosphine)palladium(0) (10.3 mg, 0.0089 mmol), copper(I) iodide (3.4 mg, 0.018 mmol), and iodobenzene (20.0 μL , 0.177 mmol). These reagents were then dissolved in anhydrous *N,N*-dimethylformamide (2.0 mL), and triethylamine (22.0 μL , 0.160 mmol) was finally added dropwise. 21 (30.8 mg, 0.089 mmol) as a 0.6 M solution in anhydrous *N,N*-dimethylformamide was added, and the reaction proceeded at room temperature for 4 h. Then, the reaction temperature was adjusted to 80 °C for an additional 3 h. Upon completion by TLC, the reaction was quenched with deionized water. The crude reaction mixture was extracted with ethyl acetate, washed with brine, and the organic layer was dried with sodium sulfate. The organic layer was filtered, concentrated in vacuo, and the crude material was purified via column chromatography using a gradient of 99:1 hexanes/triethylamine to 79.5:19.5:1 hexanes/ethyl acetate/triethylamine to afford 44 (17.0 mg, 45%) as a brown residue. ^1H NMR: (500 MHz, CDCl_3) δ 8.33 (s, 1H), 7.50 (d, $J = 7.6$ Hz, 1H), 7.38 (d, $J = 7.7$ Hz, 1H), 7.19–7.04 (m, 5H), 6.78 (d, $J = 7.6$ Hz, 2H), 4.09 (d, $J = 17.4$ Hz, 1H), 3.99 (d, $J = 17.4$ Hz, 1H), 3.38 (m, 1H), 3.34–3.24 (m, 2H), 2.99 (dt, $J = 11.0, 3.7$ Hz, 1H), 2.92–2.76 (m, 3H), 2.28 (d, $J = 17.1$ Hz, 1H), 2.00 (d, $J = 13.1$ Hz, 1H), 1.82 (q, $J = 12.3$ Hz, 1H), 1.68–1.46 (m, 2H), 1.42 (m, 1H), 1.23 (m, 1H), 0.80 (t, $J = 7.5$ Hz, 3H). ^{13}C NMR: (100 MHz, CDCl_3) δ 174.1, 137.6, 132.1, 131.8, 128.1, 128.0, 126.4, 122.9, 122.6, 119.4, 118.4, 114.6, 112.4, 84.3, 83.4, 82.5, 50.1, 49.9, 44.2, 43.9, 32.8, 30.4, 26.9, 22.3, 18.4, 9.5. HRMS (ESI): calcd for $\text{C}_{28}\text{H}_{30}\text{N}_3\text{O}$ [$\text{M} + \text{H}$] $^+$: 424.2383, found: 424.2380. $[\alpha]_{\text{D}}^{20}$: +3° (c 0.10 g/100 mL, CH_2Cl_2).

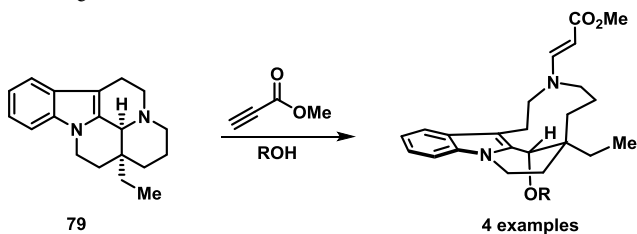


Procedure for the Chemical Synthesis of 45, (1S,17S)-3,20-Dibenzyl-17-ethyl-3,13,20-triazapentacyclo[11.7.0.0 1,17 .0 2,10 .0 4,9]jicosa-2(10),4,6,8-tetraen-19-one. To a flame-dried round-bottom flask containing anhydrous tetrahydrofuran (2.0 mL) was added sodium hydride (8.0 mg, 0.19 mmol, 60% dispersion in mineral oil). Compound 24 (38.0 mg, 0.095 mmol) was dissolved as a 0.2 M solution in anhydrous tetrahydrofuran, added to the reaction mixture at 0 °C, and allowed to stir for 15 min. After that time, 25.0 μL benzyl bromide (0.214 mmol) was added to the reaction, which was allowed to warm to room temperature and stir for an additional 12 h. After that time, an additional 2 equiv of sodium hydride (16.0 mg, 0.38 mmol, 60% dispersion in mineral oil) was added, and the reaction was heated to 66 °C for an additional 6 h. Once complete by TLC, the reaction was quenched with brine, extracted with ethyl acetate, and the organic layer was dried with sodium sulfate. The organic layer was then filtered, concentrated in vacuo, and the crude material was purified via column chromatography using a gradient of 99:1 hexanes/triethylamine to 74.5:14.5:1 hexanes/ethyl acetate/triethylamine to afford 45 (19.0 mg, 36%) as a brown residue. ^1H NMR: (500 MHz, CDCl_3) δ 7.62 (m, 1H), 7.24–7.12 (m, 5H), 7.08 (m, 1H), 7.04–6.95 (m, 4H), 6.91–6.86 (m, 3H), 4.77 (d, $J = 18.2$ Hz, 1H), 4.31 (d, $J = 18.2$ Hz,

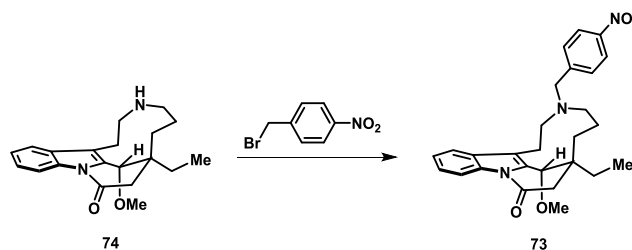
1H), 4.12 (s, 2H), 3.28 (ddd, $J = 11.5, 7.0, 4.9$ Hz, 1H), 3.20 (dt, $J = 11.9, 5.4$ Hz, 1H), 2.96 (dt, $J = 14.8, 5.1$ Hz, 1H), 2.82 (ddd, $J = 14.8, 7.6, 4.7$ Hz, 1H), 2.73 (m, 1H), 2.61 (m, 1H), 2.36 (d, $J = 18.0$ Hz, 1H), 2.21 (d, $J = 17.9$ Hz, 1H), 1.74 (m, 1H), 1.68 (m, 1H), 1.50 (m, 1H), 1.43 (m, 1H), 1.23 (m, 1H), 1.08 (sextet, $J = 7.4$ Hz, 1H), 0.42 (t, $J = 7.4$ Hz, 3H). ^{13}C NMR: (100 MHz, CDCl_3) δ 174.6, 138.9, 137.0, 136.7, 132.6, 129.8, 128.6, 128.1, 127.3, 127.1, 126.5, 125.8, 123.0, 119.8, 118.7, 116.1, 111.2, 85.1, 50.2, 47.7, 47.5, 45.7, 44.4, 42.5, 34.0, 31.5, 23.0, 17.6, 8.6. HRMS (ESI): calcd for $\text{C}_{33}\text{H}_{36}\text{N}_3\text{O}$ $[\text{M} + \text{H}]^+$: 490.2853, found: 490.2856. $[\alpha]_{\text{D}}^{20}$: $+20^\circ$ (c 0.20 g/100 mL, CH_2Cl_2).



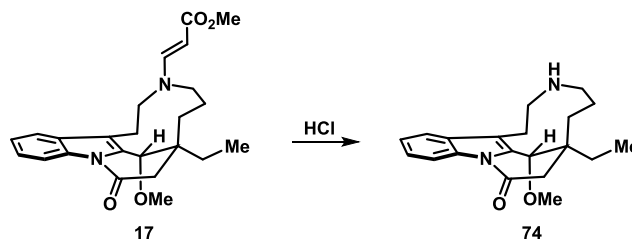
General Procedure for the Synthesis of 69–72. Compound 79 (30.1 mg, 0.107 mmol) was added to a flame-dried round-bottom flask and dissolved in chloroform (30.8 mL). Phenol (402 mg, 4.28 mmol) was added as one portion, and then methyl propiolate (14.0 μL , 0.161 mmol) was added dropwise at room temperature. The reaction was heated to 62°C for 2 h. Upon completion, the reaction was then cooled down to room temperature, quenched with saturated aqueous brine, and extracted with dichloromethane. The organic layer was dried with sodium sulfate, filtered, concentrated in vacuo, and the crude material was purified via column chromatography using a gradient of 100% hexanes to 3:1 hexanes/ethyl acetate to afford 69 (28.0 mg, 57%) as a clear solid.



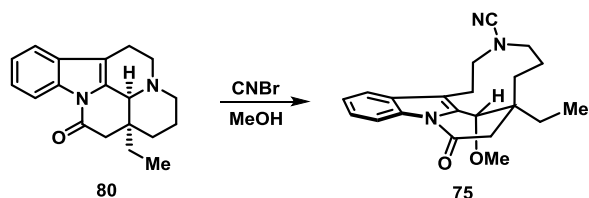
Procedure for the Synthesis of 73, (11S,19R)-11-Ethyl-19-methoxy-15-[(4-nitrophenyl)methyl]-8,15-diazatetracyclo[9.6.2.0^{2,7}.0^{8,18}]nonadeca-1(18),2,4,6-tetraen-9-one. Compound 74 (36.0 mg, 0.110 mmol) was added to a round-bottom flask. Anhydrous N,N -dimethylformamide (2.8 mL), potassium carbonate (61.0 mg, 0.440 mmol), and 4-nitrobenzyl bromide (48.0 mg, 0.220 mmol) were added sequentially at room temperature. The reaction was stirred for 2 h and, upon completion by TLC, was then quenched with brine and extracted with dichloromethane. The organic layer was then dried with sodium sulfate, filtered, concentrated in vacuo, and the crude material was purified via column chromatography using a gradient of 99:1 hexanes/triethylamine to 87:12:1 hexanes/ethyl acetate/triethylamine to afford 73 (26.3 mg, 52%) as a brown solid. ^1H NMR: (500 MHz, CD_3CN at 65°C) δ 8.40 (dt, $J = 8.3, 0.9$ Hz, 1H), 7.54 (d, $J = 8.2$ Hz, 2H), 7.35 (ddd, $J = 8.3, 7.3, 1.2$ Hz, 1H), 7.17 (dt, $J = 7.9, 0.9$ Hz, 1H), 7.04 (td, $J = 7.5, 0.9$ Hz, 1H), 6.74 (d, $J = 8.2$ Hz, 2H), 4.64 (s, 1H), 3.63 (d, $J = 14.6$ Hz, 1H), 3.23 (s, 3H), 3.19 (d, $J = 14.6$ Hz, 1H), 3.04 (ddd, $J = 14.5, 10.4, 5.9$ Hz, 1H), 2.99 (d, $J = 17.4$ Hz, 1H), 2.95–2.87 (m, 2H), 2.61 (td, $J = 12.3, 5.1$ Hz, 1H), 2.48 (ddd, $J = 12.3, 5.6, 1.2$ Hz, 1H), 2.35 (dd, $J = 17.4, 1.2$ Hz, 1H), 2.19 (dt, $J = 13.9, 3.4$ Hz, 1H), 2.02 (m, 1H), 1.75 (sextet, $J = 7.6$ Hz, 1H), 1.67–1.59 (m, 2H), 1.50 (m, 1H), 1.33 (m, 1H), 0.93 (t, $J = 7.6$ Hz, 3H). ^{13}C NMR: (100 MHz, CD_3CN at 65°C) δ 170.7, 149.0, 147.9, 136.4, 134.9, 131.0, 130.2, 126.0, 124.6, 123.8, 120.2, 120.1, 117.1, 76.8, 58.2, 56.5, 52.1, 51.7, 45.1, 42.4, 29.0, 27.0, 22.5 (2), 8.1. HRMS (ESI): calcd for $\text{C}_{27}\text{H}_{32}\text{N}_3\text{O}_4$ $[\text{M} + \text{H}]^+$: 462.2387, found: 462.2403. MP: 173 – 175°C . $[\alpha]_{\text{D}}^{20}$: $+75^\circ$ (c 0.28 g/100 mL, CH_2Cl_2).



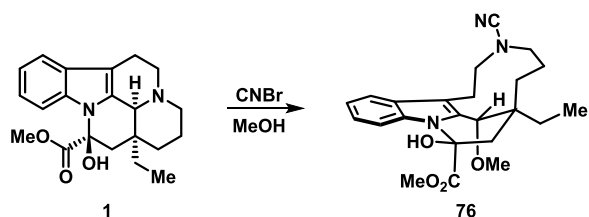
Synthesis Procedure for the Generation of 74, (11S,19R)-11-Ethyl-19-methoxy-8,15-diazatetracyclo[9.6.2.0^{2,7}.0^{8,18}]nonadeca-1(18),2,4,6-tetraen-9-one. Compound 17 (640 mg, 1.56 mmol) was added to a stirring solution of 1.0 M hydrogen chloride in methanol (15.6 mL). The reaction was allowed to stir at room temperature for 1.5 h until complete. The reaction mixture was then diluted with brine and extracted with ethyl acetate. The organic layer was collected via separatory funnel, dried with sodium sulfate, filtered, and concentrated in vacuo. The crude material was then purified via column chromatography using a gradient of 99:1 hexanes/triethylamine to 74.5:24.5:1 hexanes/ethyl acetate/triethylamine to 99:1 ethyl acetate/triethylamine to afford 74 (503 mg, 99%) as a clear-yellow residue. ^1H NMR: (400 MHz, CDCl_3) δ 8.42 (d, $J = 8.0$ Hz, 1H), 7.45 (d, $J = 7.5$ Hz, 1H), 7.34–7.19 (m, 2H), 4.69 (s, 1H), 3.15 (s, 3H), 3.00 (d, $J = 17.3$ Hz, 1H), 3.00–2.89 (m, 2H), 2.82 (dd, $J = 13.7, 4.0$ Hz, 1H), 2.78–2.66 (m, 2H), 2.32 (d, $J = 17.3$ Hz, 1H), 2.32 (m, 1H), 1.98 (sextet, $J = 7.6$ Hz, 1H), 1.62–1.50 (m, 2H), 1.39–1.33 (m, 2H), 1.03 (m, 1H), 0.84 (t, $J = 7.6$ Hz, 3H), 0.74 (m, 1H). ^{13}C NMR: (100 MHz, CDCl_3) δ 169.3, 135.1, 133.7, 128.9, 125.1, 123.5, 118.5, 117.8, 116.5, 75.3, 55.8, 45.7, 45.4, 43.5, 41.2, 28.8, 25.6, 23.8, 22.4, 7.5. HRMS (ESI): calcd for $\text{C}_{20}\text{H}_{27}\text{N}_2\text{O}_2$ $[\text{M} + \text{H}]^+$: 327.2067, found: 327.2082. $[\alpha]_{\text{D}}^{20}$: $+17^\circ$ (c 0.67 g/100 mL, CH_2Cl_2). Note: 74 is the synthetic precursor to 5.



Procedure for the Chemical Synthesis of 75, (11S,19R)-11-Ethyl-19-methoxy-9-oxo-8,15-diazatetracyclo[9.6.2.0^{2,7}.0^{8,18}]nonadeca-1(18),2,4,6-tetraene-15-carbonitrile. Compound 80 (89.0 mg, 0.302 mmol) was added to a flame-dried round-bottom flask and dissolved in a (2:1) chloroform/methanol solution (6.6 mL). A 3.0 M solution of cyanogen bromide in dichloromethane (0.30 mL, 0.906 mmol) was added dropwise to the mixture, and the resulting reaction was allowed to stir at room temperature for 21 h. Upon completion by TLC, the reaction mixture was quenched with brine and extracted with dichloromethane. The organic layer was collected and dried with sodium sulfate, filtered, and concentrated in vacuo. The crude material was purified via column chromatography using a gradient of 100% hexanes, 3:1 hexanes/ethyl acetate, and 100% ethyl acetate to afford 75 (54.5 mg, 51%) as a brown residue. ^1H NMR: (400 MHz, CDCl_3) δ 8.46 (d, $J = 8.1$ Hz, 1H), 7.47 (d, $J = 7.5$ Hz, 1H), 7.39 (td, $J = 8.1, 1.2$ Hz, 1H), 7.32 (td, $J = 7.5, 1.2$ Hz, 1H), 4.45 (s, 1H), 3.77 (dt, $J = 13.9, 3.0$ Hz, 1H), 3.45 (ddd, $J = 13.1, 7.4, 1.7$ Hz, 1H), 3.29 (s, 3H), 3.09–3.02 (m, 3H), 2.82 (m, 1H), 2.40 (dd, $J = 17.4, 1.3$ Hz, 1H), 2.24 (dd, $J = 13.1, 8.6$ Hz, 1H), 2.10 (sextet, $J = 7.6$ Hz, 1H), 1.86–1.58 (m, 4H), 0.91 (m, 1H), 0.88 (t, $J = 7.6$ Hz, 3H). ^{13}C NMR: (100 MHz, CDCl_3) δ 169.4, 135.2, 133.9, 128.6, 126.0, 124.1, 118.0, 117.4, 117.2, 117.1, 75.5, 56.5, 55.2, 54.0, 43.5, 41.0, 32.8, 26.2, 23.1, 21.5, 7.9. HRMS (ESI): calcd for $\text{C}_{21}\text{H}_{26}\text{N}_3\text{O}_2$ $[\text{M} + \text{H}]^+$: 352.2020, found: 352.2025. $[\alpha]_{\text{D}}^{20}$: $+52^\circ$ (c 0.44 g/100 mL, CH_2Cl_2).

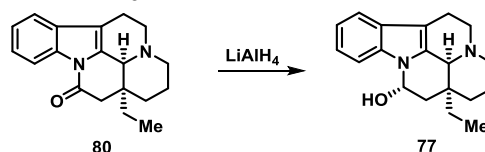


Procedure for the Synthesis of 76, Methyl (9*S*,11*S*,19*R*)-15-Cyano-11-ethyl-9-hydroxy-19-methoxy-8,15-diazatetracyclo[9.6.2.0^{2,7}.0^{8,18}]nonadeca-1(18),2,4,6-tetraene-9-carboxylate. Vincamine **1** (139.9 mg, 0.395 mmol) was added to a flame-dried round-bottom flask and subsequently dissolved in a (2:1) chloroform/methanol solution (7.3 mL). A 3.0 M solution of cyanogen bromide in dichloromethane (0.39 mL, 1.18 mmol) was added to the mixture dropwise, and the reaction was stirred at room temperature for 4 h. Upon completion by TLC, the reaction mixture was quenched with brine and extracted with dichloromethane. The organic layer was collected and dried with sodium sulfate, filtered, and concentrated in vacuo. The crude material was then purified via column chromatography using a gradient of 100% chloroform to 24:1 chloroform/acetone to afford **76** (68.0 mg, 42%) as a white solid. ¹H NMR: (400 MHz, CDCl₃) δ 7.52 (d, *J* = 7.3 Hz, 1H), 7.23–7.13 (m, 3H), 4.70 (s, 1H), 4.55 (s, 1H), 3.84 (s, 3H), 3.79 (dt, *J* = 13.7, 2.9 Hz, 1H), 3.53 (dd, *J* = 13.1, 6.4 Hz, 1H), 3.35 (s, 3H), 3.16 (ddd, *J* = 15.3, 12.3, 3.1 Hz, 1H), 3.06 (dt, *J* = 13.7, 2.9 Hz, 1H), 2.80 (d, *J* = 13.8 Hz, 1H), 2.68 (td, *J* = 15.3, 3.1 Hz, 1H), 2.08 (dd, *J* = 13.1, 6.4 Hz, 1H), 1.98–1.85 (m, 3H), 1.82–1.67 (m, 2H), 1.59 (m, 1H), 1.30 (dd, *J* = 15.9, 8.2 Hz, 1H), 0.89 (t, *J* = 7.6 Hz, 3H). ¹³C NMR: (100 MHz, CDCl₃) δ 174.8, 135.3, 133.7, 127.9, 123.1, 120.6, 118.4, 117.9, 112.1, 111.9, 83.0, 75.5, 56.8, 56.4, 55.4, 54.5, 41.0, 40.6, 32.6, 26.8, 23.5, 21.4, 8.1. HRMS (ESI): calcd for C₂₃H₂₉N₃O₄Na [M + Na]⁺: 434.2050, found: 434.2068. MP: 241–243 °C. [α]_D²⁰: +120° (c 0.25 g/100 mL, CH₂Cl₂).

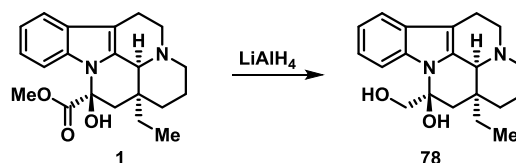


Procedure for the Synthesis of 77, (15*S*,17*S*,19*S*)-15-Ethyl-1,11-diazapentacyclo[9.6.2.0^{2,7}.0^{8,18}.0^{15,19}]nonadeca-2,4,6,8(18)-tetraen-17-ol. Lithium aluminum hydride (135 mg, 3.57 mmol) was added to tetrahydrofuran (7.14 mL) at 0 °C. Compound **80** (210 mg, 0.714 mmol) was then added portionwise to the reaction mixture at 0 °C. The reaction mixture was then allowed to warm to room temperature for approximately 2 min before heating to reflux for 1 h. Upon completion (by TLC), the reaction was quenched with 1 M sodium hydroxide (five to six drops) and distilled water (1 mL). The crude mixture was filtered through celite, which was rinsed with warm ethyl acetate. The filtrate was then dried with sodium sulfate, filtered, and concentrated in vacuo. The crude product was purified via column chromatography 99:1 hexanes/triethylamine to 79.5:19.5:1 hexanes/ethyl acetate/triethylamine to afford **77** (179 mg, 84%) as a white powder. Note: **77** is a known compound (CAS No. 19877-90-8). Spectral data for select (diagnostic) ¹H and ¹³C signals are reported in the literature;³⁹ however, we reported the full tabulated data and HRMS for this compound below. ¹H NMR: (400 MHz, CDCl₃) δ 7.79 (d, *J* = 7.7 Hz, 1H), 7.49 (dd, *J* = 7.5, 0.9 Hz, 1H), 7.23–7.16 (m, 2H), 5.52 (br s, 1H), 5.47 (dd, *J* = 9.8, 4.9 Hz, 1H), 3.21 (s, 1H), 3.15 (dd, *J* = 13.1, 6.0 Hz, 1H), 3.01 (td, *J* = 12.7, 6.2 Hz, 1H), 2.89 (m, 1H), 2.47–2.41 (m, 2H), 2.26 (td, *J* = 12.0, 2.9 Hz, 1H), 2.12 (dd, *J* = 14.1, 4.6 Hz, 1H), 1.96 (sextet, *J* = 7.5 Hz, 1H), 1.62 (m, 1H), 1.41 (dd, *J* = 13.6, 9.6 Hz, 1H), 1.34–1.21 (m, 3H), 0.84 (t, *J* = 7.5 Hz, 3H), 0.76 (td, *J* = 13.7, 3.8 Hz, 1H). ¹³C NMR: (100 MHz, CDCl₃) δ 136.9, 132.7, 128.7, 121.2, 120.1, 118.1, 112.4, 105.2, 76.5, 58.5, 50.7, 44.3, 43.0, 36.7, 28.5, 24.8, 20.4, 16.9, 7.7. HRMS (ESI): calcd for

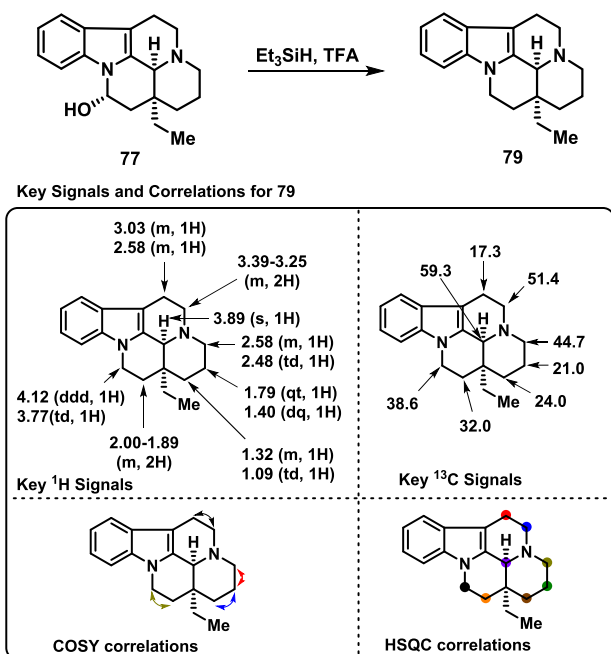
C₁₉H₂₅N₂O [M + H]⁺: 297.1961, found: 297.1966. MP: 83–85 °C. [α]_D²⁰: +73° (c 0.15 g/100 mL, CH₂Cl₂).



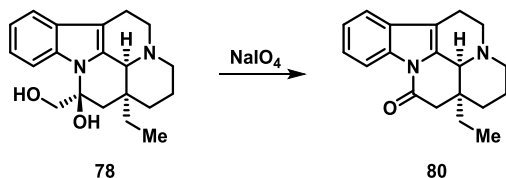
Procedure for the Synthesis of 78, (15*S*,17*S*,19*S*)-15-Ethyl-17-(hydroxymethyl)-1,11-diazapentacyclo[9.6.2.0^{2,7}.0^{8,18}.0^{15,19}]nonadeca-2,4,6,8(18)-tetraen-17-ol. Lithium aluminum hydride (2.69 g, 70.8 mmol) was added to a solution of tetrahydrofuran (142 mL) in a round-bottom flask at 0 °C. Vincamine **1** (5.02 g, 14.2 mmol) was then added portionwise at 0 °C before allowing to warm to room temperature. The reaction mixture was then heated to 66 °C and allowed to stir for 1.5 h. After that time, the reaction was cooled and then quenched with 1 M sodium hydroxide (aqueous solution, 2 mL), followed by the addition of distilled water (10 mL). The resulting mixture was then filtered through a frit funnel containing celite. The filtrate was then rinsed with warm ethyl acetate. The organic solution containing the product was dried with sodium sulfate and concentrated in vacuo to afford **78** (4.17 g, 99%) as a yellow-white solid. Note: **78** is a known compound (CAS No. 3382-95-4).⁴⁰ ¹H NMR: (400 MHz, CDCl₃) δ 7.63 (m, 1H), 7.48 (m, 1H), 7.17–7.09 (m, 2H), 4.10 (d, *J* = 11.4 Hz, 1H), 3.87 (d, *J* = 11.4 Hz, 1H), 3.71 (s, 1H), 3.28–2.69 (m, 4H), 2.55–2.47 (m, 2H), 2.33 (td, *J* = 12.3, 3.0 Hz, 1H), 2.26–2.13 (m, 2H), 2.04 (d, *J* = 15.1 Hz, 1H), 1.69 (m, 1H), 1.49 (m, 1H), 1.37 (sextet, *J* = 7.1 Hz, 1H), 1.32–1.22 (m, 3H), 0.91 (t, *J* = 7.5 Hz, 3H). ¹³C NMR: (100 MHz, CDCl₃) δ 134.0, 132.4, 129.3, 121.3, 120.1, 118.6, 112.7, 105.7, 84.8, 67.6, 59.5, 50.8, 44.3, 44.2, 34.5, 28.9, 25.9, 20.8, 16.9, 7.8. MP: 180–182 °C, lit. 180–182 °C.⁴⁰ [α]_D²⁰: +10° (c 0.17 g/100 mL, CH₂Cl₂), lit. +10.6 (CHCl₃, c 1.0 g/100 mL, pyridine).⁴⁰ Note: Compound **78** is an intermediate en route to **12** and **17**.



Procedure for the Synthesis of 79, (15*S*,19*S*)-15-Ethyl-1,11-diazapentacyclo[9.6.2.0^{2,7}.0^{8,18}.0^{15,19}]nonadeca-2,4,6,8(18)-tetraene. Compound **77** (70.2 mg, 0.237 mmol) was added to a round-bottom flask. Anhydrous dichloromethane (2.4 mL), triethylsilane (2.1 mL, 13.0 mmol), and trifluoroacetic acid (0.472 mL, 6.2 mmol) were added to the flask sequentially. The reaction was stirred for 2 h, then quenched with saturated aqueous sodium bicarbonate, washed with brine, and extracted with dichloromethane. Then, the organic layer was dried with sodium sulfate, filtered, and the organic layer was concentrated in vacuo. The crude product was purified via column chromatography 99:1 hexanes/triethylamine to 82.5:16.5:1 hexanes/ethyl acetate/triethylamine to afford **79** (53.0 mg, 80%) as a colorless residue. Note: **79** is a known compound⁴¹ (CAS No. 65026-49-5). ¹H NMR: (400 MHz, CDCl₃) δ 7.55 (m, 1H), 7.32 (ddd, *J* = 8.0, 1.2, 0.8 Hz, 1H), 7.22 (td, *J* = 7.5, 1.2 Hz, 1H), 7.16 (ddd, *J* = 8.1, 7.0, 1.3 Hz, 1H), 4.12 (ddd, *J* = 11.8, 5.9, 1.9 Hz, 1H), 3.89 (s, 1H), 3.77 (td, *J* = 12.0, 5.2 Hz, 1H), 3.39–3.25 (m, 2H), 3.03 (m, 1H), 2.65–2.55 (m, 2H), 2.48 (td, *J* = 12.6, 3.1 Hz, 1H), 2.17 (sextet, *J* = 7.6 Hz, 1H), 2.03–1.73 (m, 3H), 1.58 (sextet, *J* = 7.5 Hz, 1H), 1.40 (m, 1H), 1.32 (m, 1H), 1.09 (td, *J* = 13.3, 4.1 Hz, 1H), 0.97 (t, *J* = 7.6 Hz, 3H). ¹³C NMR: (100 MHz, CDCl₃) δ 136.4, 132.9, 128.2, 120.6, 119.4, 118.2, 109.4, 104.5, 59.3, 51.4, 44.7, 38.6, 34.2, 32.0, 29.1, 24.0, 21.0, 17.3, 7.7. HRMS (ESI): calcd for C₁₉H₂₅N₂ [M + H]⁺: 281.2012, found: 281.2008. [α]_D²⁰: -6° (c 0.24 g/100 mL, CH₂Cl₂); lit. [α]_D²⁰: -11.7° (c 0.2, CH₂Cl₂).⁴¹

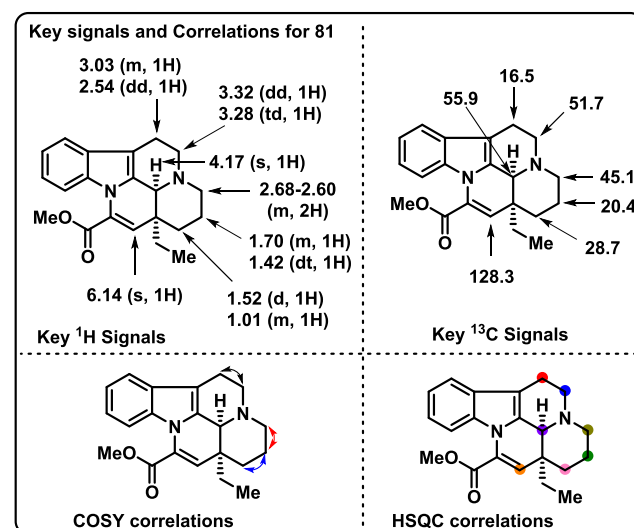
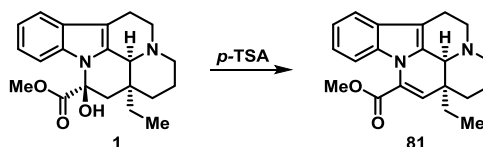


Procedure for the Synthesis of 80, (15S,19S)-15-Ethyl-1,11-diazapentacyclo[9.6.2.0^{2,7}.0^{8,18}.0^{15,19}]nonadeca-2,4,6,8(18)-tetraen-17-one. Compound 78 (4.17 g, 12.8 mmol) was added to a round-bottom flask and dissolved in 3:1 solution of tetrahydrofuran/water (128 mL). Sodium periodate (13.7 g, 64.0 mmol) was added portionwise, and the reaction was stirred at room temperature for 4 h. The reaction was quenched with saturated aqueous sodium thiosulfate, extracted with ethyl acetate, and the extract was dried with sodium sulfate. The crude extract was concentrated in vacuo to yield 80 (3.69 g, 93%) as a brownish-white solid. Note: 80 is a known compound (CAS No. 4880-88-0).^{40,42,43} ¹H NMR: (400 MHz, CDCl₃) δ 8.37 (m, 1H), 7.42 (m, 1H), 7.35–7.27 (m, 2H), 3.96 (s, 1H), 3.33 (dd, *J* = 13.9, 6.5 Hz, 1H), 3.23 (ddd, *J* = 13.9, 11.3, 5.8 Hz, 1H), 2.90 (dddd, *J* = 16.7, 11.2, 6.7, 2.9 Hz, 1H), 2.66 (d, *J* = 16.7 Hz, 1H), 2.59 (d, *J* = 16.7 Hz, 1H), 2.58 (m, 1H), 2.47 (dd, *J* = 17.0, 2.5 Hz, 1H), 2.42 (td, *J* = 11.5, 3.3 Hz, 1H), 2.04 (sextet, *J* = 7.7 Hz, 1H), 1.74 (m, 1H), 1.65 (sextet, *J* = 7.6 Hz, 1H), 1.49 (td, *J* = 13.8, 2.0 Hz, 1H), 1.38 (dp, *J* = 13.1, 3.1 Hz, 1H), 1.03 (td, *J* = 13.5, 3.9 Hz, 1H), 0.93 (t, *J* = 7.6 Hz, 3H). ¹³C NMR: (100 MHz, CDCl₃) δ 167.4, 134.0, 132.0, 130.0, 124.0, 123.7, 117.9, 116.0, 112.1, 57.1, 50.3, 44.1, 43.9, 38.0, 28.1, 26.7, 20.5, 16.3, 7.6. MP: 168–170 °C, lit. 173⁴⁰ and 166–168 °C.⁴² [α]_D²⁰: –94° (c 0.24 g/100 mL, CH₂Cl₂), lit. –90° (c 1.0 g/100 mL, CHCl₃).⁴⁰ Note: Compound 80 is an intermediate en route to 12 and 17.

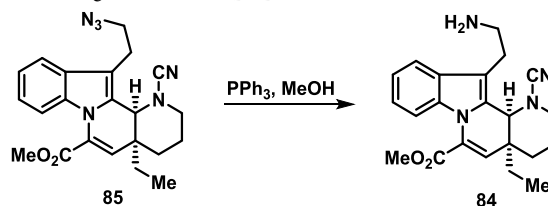


Synthesis Procedure for the Generation of 81, Methyl (15S,19S)-15-Ethyl-1,11-diazapentacyclo[9.6.2.0^{2,7}.0^{8,18}.0^{15,19}]nonadeca-2,4,6,8(18),16-pentaene-17-carboxylate. Vincamine 1 (5.1 g, 14.4 mmol) was added to a round-bottom flask and dissolved in toluene (48 mL). *p*-Toluenesulfonic acid monohydrate (5.5 g, 28.8 mmol) was added to the solution, and the flask was equipped with a Dean–Stark trap and heated at reflux for 2 h. Upon completion of the reaction (monitored by TLC), the mixture was basified to pH 6–7 with a 1 M aqueous sodium hydroxide solution and then extracted with ethyl acetate. The organic layer was collected and dried with sodium sulfate, filtered, and concentrated in vacuo. The crude material was then purified via column chromatography using a 99:1 hexanes/triethylamine to 49.5:49.5:1 hexanes/ethyl acetate/triethylamine to afford 81 (4.5 g, 95%) as a light yellow solid. Note: 81 is a known compound

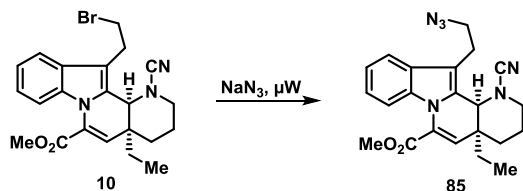
(apovincamine, CAS No. 4880-92-6),^{44,45} and this procedure converting vincamine to 81 was adapted from the literature.⁴⁴ ¹H NMR: (600 MHz, CDCl₃) δ 7.47 (d, *J* = 7.7 Hz, 1H), 7.23 (d, *J* = 8.3 Hz, 1H), 7.17 (td, *J* = 7.1, 1.1 Hz, 1H), 7.13 (td, *J* = 7.2, 0.9 Hz, 1H), 6.14 (s, 1H), 4.17 (s, 1H), 3.95 (s, 3H), 3.38 (dd, *J* = 13.9, 6.2 Hz, 1H), 3.27 (td, *J* = 11.7, 5.5 Hz, 1H), 3.03 (m, 1H), 2.70–2.60 (m, 2H), 2.54 (dd, *J* = 16.4, 3.4 Hz, 1H), 2.00–1.86 (m, 2H), 1.75 (m, 1H), 1.52 (d, *J* = 13.7 Hz, 1H), 1.42 (dt, *J* = 13.2, 2.9 Hz, 1H), 1.06–0.98 (m, 4H). ¹³C NMR: (150 MHz, CDCl₃) δ 164.0, 134.3, 130.9, 129.2, 128.4, 128.3, 122.2, 120.5, 118.5, 112.6, 108.9, 56.0, 52.7, 51.7, 45.1, 38.0, 28.7, 27.5, 20.4, 16.5, 8.9. MP: 159–161 °C. [α]_D²⁰: +112° (c 0.61 g/100 mL, CH₂Cl₂), lit. +98° (c 0.51 g/100 mL, MeOH).⁴⁵ Note: Compound 81 is an intermediate en route to 10.



Procedure for the Chemical Synthesis of 84, Methyl (4aS,12bS)-12-(2-Aminoethyl)-1-cyano-4a-ethyl-1H,2H,3H,4H,4aH,12bH-indolo[1,2-h]1,7-naphthyridine-6-carboxylate. Compound 85 (157 mg, 0.388 mmol) was added to a flame-dried round-bottom flask and dissolved in methanol (6.50 mL). Triphenylphosphine (153 mg, 0.582 mmol) was then added to the resulting solution, and the reaction mixture was heated to reflux. The reaction proceeded for 1 h before being cooled down to room temperature and concentrated in vacuo. The crude material was purified by column chromatography using a gradient of 99:1 ethyl acetate/triethylamine to 89.5:9.5:1 ethyl acetate/methanol:triethylamine to yield 84 (122 mg, 83%) as a clear residue. ¹H NMR: (400 MHz, CDCl₃) δ 7.59 (d, *J* = 7.8 Hz, 1H), 7.23–7.09 (m, 3H), 6.12 (d, *J* = 1.7 Hz, 1H), 4.13 (d, *J* = 1.7 Hz, 1H), 3.92 (s, 3H), 3.38 (d, *J* = 12.2 Hz, 1H), 3.17–2.86 (m, 5H), 2.18 (s, 2H), 2.03 (d, *J* = 13.2 Hz, 1H), 1.81–1.61 (m, 2H), 1.35 (td, *J* = 14.0, 4.2 Hz, 1H), 0.99 (q, *J* = 7.5 Hz, 2H), 0.67 (t, *J* = 7.5 Hz, 3H). ¹³C NMR: (100 MHz, CDCl₃) δ 163.5, 134.8, 130.2, 128.7, 127.8, 127.2, 123.8, 121.0, 119.7, 118.2, 116.7, 112.5, 56.6, 52.7, 49.9, 42.4, 39.5, 32.3, 31.4, 28.1, 21.8, 8.0. HRMS (ESI): calcd for C₂₂H₂₆N₄O₂Na [M + Na]⁺: 401.1948, found: 401.1962. [α]_D²⁰: –66° (c 0.38 g/100 mL, CH₂Cl₂).



Procedure for the Chemical Synthesis of 85, Methyl (4a*S*,12*bS*)-12-(2-Azidoethyl)-1-cyano-4*a*-ethyl-1*H*,2*H*,3*H*,4*H*,4*aH*,12*bH*-indolo[1,2-*h*]1,7-naphthyridine-6-carboxylate. Compound **10** (256 mg, 0.579 mmol) was added to a flame-dried microwave flask and dissolved in *N,N*-dimethylformamide (6.00 mL). Sodium azide (301 mg, 4.63 mmol) was then added to the resulting solution, and the reaction mixture was subjected to microwave irradiation at 100 °C for 6 min. Upon completion of this reaction (monitored by TLC), the reaction was cooled down to room temperature, diluted with ethyl acetate, and quenched with brine. The organic layer was collected and dried with sodium sulfate, filtered, and concentrated in vacuo. The crude material was finally purified via column chromatography using a gradient of 100% chloroform to 99:1 chloroform/acetone to yield **85** (174 mg, 73%) as a white solid. ¹H NMR: (400 MHz, CDCl₃) δ 7.58 (m, 1H), 7.26 (m, 1H), 7.23–7.15 (m, 2H), 6.15 (d, *J* = 1.7 Hz, 1H), 4.11 (d, *J* = 1.7 Hz, 1H), 3.96 (s, 3H), 3.72 (ddd, *J* = 12.2, 8.2, 5.7 Hz, 1H), 3.61 (ddd, *J* = 12.2, 7.9, 4.1 Hz, 1H), 3.48 (dp, *J* = 10.3, 2.1 Hz, 1H), 3.21–3.03 (m, 3H), 2.13 (dt, *J* = 13.8, 3.5 Hz, 1H), 1.89–1.70 (m, 2H), 1.42 (td, *J* = 13.2, 4.2 Hz, 1H), 1.17–1.01 (m, 2H), 0.75 (t, *J* = 7.5 Hz, 3H). Note: ¹H spectrum referenced TMS at 0.00 ppm. ¹³C NMR: (100 MHz, CDCl₃) δ 163.4, 134.7, 130.1, 128.2, 128.1, 127.4, 124.0, 121.2, 119.3, 116.7, 116.6, 112.7, 56.8, 52.8, 51.5, 50.1, 39.4, 32.3, 31.4, 24.4, 21.8, 8.1. HRMS (ESI): calcd for C₂₂H₂₄N₆O₂Na [M + Na]⁺: 427.1853, found: 427.1860. MP: 41–43 °C. [α]_D²⁰: –32° (c 0.30 g/100 mL, CH₂Cl₂).



Biology. In Vitro Screening against GPCR Drug Targets and Dose–Response Experiments (Performed at DiscoverX). PathHunter β-Arrestin Assays. PathHunter cell lines were expanded from freezer stocks according to standard procedures. Cells were seeded in a total volume of 20 μL into white-walled, 384-well microplates and incubated at 37 °C prior to testing. For agonist determination, cells were incubated with a sample to induce a response. Intermediate dilution of sample stocks was performed to generate a 5× sample in assay buffer. 5 μL of 5× sample was added to cells and incubated at 37 °C or room temperature for 90 or 180 min. The final assay vehicle concentration was 1%. For antagonist determination, cells were preincubated with an antagonist followed by agonist challenge at the EC₈₀ concentration. The intermediate dilution of sample stocks was performed to generate a 5× sample in assay buffer. 5 μL of 5× sample was added to cells and incubated at 37 °C or room temperature for 30 min. Vehicle concentration was 1%. 5 μL of a 6× EC₈₀ agonist in assay buffer was added to the cells and incubated at 37 °C or room temperature for 90 or 180 min. Assay signal was generated through a single addition of 12.5 or 15 μL (50% v/v) of PathHunter Detection reagent cocktail, followed by a 1 h incubation at room temperature. Microplates were read following signal generation with a PerkinElmer Envision instrument for chemiluminescent signal detection. Compound activity was analyzed using CBIS data analysis suite (ChemInnovation, CA). For agonist mode assays, the percentage activity was calculated using the following formula: % Activity = 100% × (mean RLU of test sample – mean RLU of vehicle control)/(mean MAX control ligand – mean RLU of vehicle control). For antagonist mode assays, the percentage inhibition was calculated using the following formula: % Inhibition = 100% × (1 – (mean RLU of test sample – mean RLU of vehicle control)/(mean RLU of EC80 control – mean RLU of vehicle control)). Note: protocol from DiscoverX. Dose–response experiments (antagonists) were carried out in assays analogous to the initial screen against GPCRs. Dose–response curves for all IC₅₀ values obtained during these studies can be found in the [Supporting Information](#).

Animal Experiments. Morphine (Sigma-Aldrich) utilized in place-conditioning experiments was used under experiments approved by the UF EH&S, under the auspices of Dr. Jay P. McLaughlin's DEA

license (RM0398176). Powdered morphine stock was kept in the dark at room temperature under lock-and-key, and quantities prepared for use on each day needed were recorded as per U.S. Federal Regulation as maintained by the Drug Enforcement Administration.

Animals and Housing. All animal studies were preapproved by the Institutional Animal Care and Use Committee (under IACUC protocol 201910772) at the University of Florida (Gainesville, FL), in accordance with the 1996 National Institute of Health Guide for the Care and Use of Laboratory Animals. Male C57BL/6J mice (Jackson Labs, Bar Harbor, ME) weighing 20–33 g and ranging from 7 to 11 weeks of age were used in these experiments. Mice were inspected regularly by veterinary staff to ensure compliance. Animals used in this study were housed and cared for in the ACS Communicore vivarium at the University of Florida in accordance with the National Institutes of Health and Animal Care and Use Center institutional guidelines.

Route of Administration. Morphine was dissolved in saline (0.9%). **4 (V2a)** was solubilized in a vehicle of 10% Solutol HS 15/90% saline (0.9%), which itself was shown to have no behavioral effect in mice. Once solubilized, the administration of **4 (V2a)** proceeded by the intracerebroventricular (i.c.v.) route [and intraperitoneal (i.p.) route for morphine].

Conditioned Place Preference Experiments. C57BL/6J wild-type mice were used in place-conditioning studies using a three-compartment box, similar to methods utilized previously.^{34–36,46,47} Place preference was determined in a 30 min test of the animal's movement through the apparatus, with location recorded automatically. Animals were pretreated with vehicle (10% Solutol HS 15/90% 0.9% saline) or **4 (V2a)** through the i.c.v. route, ±morphine (10 mg/kg, i.p.), and consistently confined for 40 min in the appropriately paired outer compartment. Place conditioning with CPP vehicle (0.9% saline, i.p.) followed 4 h later, but paired to the other outer chamber. A counterbalanced CPP design was utilized, as it yields reproducible results across studies^{48,49} and may more easily examine both conditioned place preference and aversion. A dose of 10 mg/kg i.p. morphine was selected with a 40 min conditioning period for these studies as these conditions produce reliable CPP in C57BL/6J mice with 2 days of conditioning. For experiments examining the effect of **4 (V2a)** alone, the conditioning cycle was performed 2 sequential days. For experiments of extinction and reinstatement (see the next paragraph), the conditioning cycle with morphine was performed for 4 days.^{35,36,46,47}

Extinction. Preference tests were completed twice weekly until extinction was established over a 7 week period. Extinction is defined as a statistically significant decrease in the time spent in the morphine-paired compartment as compared with the postconditioning response after 4 days of morphine place conditioning.³⁵

Reinstatement. Following the demonstration of extinction, reinstatement of morphine-CPP was examined after exposure to forced swimming (FST; see below).³⁵ Tested mice were treated on days 50 and 51 with either vehicle (50% DMSO) or **4 (V2a)** (60 nmol, i.c.v.), 15 min before forced swimming. Mice so exposed were then tested for place preference on day 52.

Forced Stress Test. To induce stress, C57BL/6J mice were exposed to a modified forced swim test (FST). Testing was performed on the basis of methods previously described.^{35,36,46,47} The modified Porsolt forced swim test paradigm used was a 2 day procedure, in which mice swam without the opportunity to escape. In all trials, mice were placed in an opaque 5 L beaker (40 cm tall × 25 cm in diameter) filled with 3.5 L of 30 °C water. After the trial, mice were removed, dried with towels, and returned to their home cages for at least 7 min before further testing. On day 1, animals were placed in water to swim for a single trial of 15 min. On day 2, animals were again placed in water to swim but through a series of four trials, each 6 min long; trials were separated by a 7–12 min return to a home cage. Multiple trials were used to induce the effects of extended exposure to the inescapable stressor. Difficulty in swimming or staying afloat was the criterion for exclusion; however, no mice met these criteria in this study. When mice were pretreated with a drug, experiments were performed with the experimenter blind to the pretreatment.

Data Analysis. CPP data are presented as the difference in the time spent in drug- and vehicle-associated chambers. All data were analyzed with Student's *t* tests or by repeated-measures two-way ANOVA as appropriate. Significant results demonstrated by ANOVA were further analyzed for significance with Tukey's honestly significant difference (HSD) post hoc test to assess group differences.⁵⁴ For all repeated measures ANOVA, simple main effects and simple main effect contrasts are presented following significant interactions, with the difference in the time spent on the treatment- vs vehicle-associated side as the dependent measure and conditioning status as the between-groups factor. Effects were considered significant when *P* < 0.05. All effects are expressed as mean ± standard error of the mean (SEM).

Molecular Modeling. Structure Preparation. The three-dimensional (3-D) structure of **4** (**V2a**) was prepared by LigPrep (Schrödinger, LLC). The human OX2 orexin receptor (hypocretin receptor 2) structures were obtained from Protein Data Bank under the codes 4S0V and 5WQC. The protein structures were pretreated with Protein Preparation Wizard (Schrödinger, LLC) to assign proper protonation states for residues. The cocrystallized ligands, water molecules, and additives were removed.

Docking with AutoDock4.2.⁵⁰ Gasteiger charges were added onto both receptor and ligand atoms. A grid box was centered at where the cocrystallized ligand is (1) Suvorexant in 4S0V structure and (2) EMPA in 5WQC structure, respectively. Dimensions of the box were set to 76 × 76 × 70 grid points with a spacing of 0.375 Å. Lamarckian genetic algorithm (LGA) was used as the search method. All docked conformations were clustered at an RMSD of 1.5 Å.

Docking with Glide SP⁵¹ and Glide XP⁵² (Schrödinger, LLC). The grid box center was set as the same as the one used in AutoDock4.2. The outer box dimensions were set to 30 Å × 30 Å × 30 Å, and the inner box dimensions were set to 10 Å × 10 Å × 10 Å. The precision mode was set to either SP or XP. At most, three conformations were required to report. All dockings were performed using the Maestro suite (release of 2016-04).

■ ASSOCIATED CONTENT

Supporting Information

The Supporting Information is available free of charge at <https://pubs.acs.org/doi/10.1021/acs.jmedchem.9b01924>.

Supporting figures, supporting (synthetic) schemes, full characterization data [¹H, ¹³C NMR, and two-dimensional (2-D) NMR spectra, high-resolution mass spectra, melting points for solids, observed color and state of compounds] for new compounds, X-ray analyses for select compounds, dose–response curves for active GPCR antagonists, acid stability assessment of **4** (**V2a**), and LC–MS traces of select compounds (PDF)

Molecular formula strings file (CSV)

Accession Codes

The authors will release the atomic coordinates and experimental data upon article publication. X-ray structures for **6** (**V1p**), **17** (**V3r**), **18** (**V3l**), and **25** (**V2i**) were obtained and submitted to the Cambridge Crystallographic Data Center (CCDC) website (CCDC codes: **6** (**V1p**), 1584222; **17** (**V3r**), 1584221; **18** (**V3l**), 1584220; and **25** (**V2i**), 1848065).

■ AUTHOR INFORMATION

Corresponding Author

Robert W. Huigens, III – Department of Medicinal Chemistry, College of Pharmacy and Center for Natural Products, Drug Discovery & Development (CNP3), College of Pharmacy, University of Florida, Gainesville, Florida 32610, United States; orcid.org/0000-0003-3811-2721; Phone: (352) 273-7718; Email: rhuigens@cop.ufl.edu

Authors

Verrill M. Norwood, IV – Department of Medicinal Chemistry, College of Pharmacy and Center for Natural Products, Drug Discovery & Development (CNP3), College of Pharmacy, University of Florida, Gainesville, Florida 32610, United States

Ariana C. Brice-Tutt – Department of Pharmacodynamics, College of Pharmacy and Center for Natural Products, Drug Discovery & Development (CNP3), College of Pharmacy, University of Florida, Gainesville, Florida 32610, United States

Shannel O. Eans – Department of Pharmacodynamics, College of Pharmacy and Center for Natural Products, Drug Discovery & Development (CNP3), College of Pharmacy, University of Florida, Gainesville, Florida 32610, United States

Heather M. Stacy – Department of Pharmacodynamics, College of Pharmacy and Center for Natural Products, Drug Discovery & Development (CNP3), College of Pharmacy, University of Florida, Gainesville, Florida 32610, United States

Guqin Shi – Department of Medicinal Chemistry, College of Pharmacy and Center for Natural Products, Drug Discovery & Development (CNP3), College of Pharmacy, University of Florida, Gainesville, Florida 32610, United States

Ranjala Ratnayake – Department of Medicinal Chemistry, College of Pharmacy and Center for Natural Products, Drug Discovery & Development (CNP3), College of Pharmacy, University of Florida, Gainesville, Florida 32610, United States

James R. Rocca – Department of Medicinal Chemistry, College of Pharmacy and McKnight Brain Institute, University of Florida, Gainesville, Florida 32610, United States

Khalil A. Abboud – Department of Chemistry, University of Florida, Gainesville, Florida 32610, United States

Chenglong Li – Department of Medicinal Chemistry, College of Pharmacy and Center for Natural Products, Drug Discovery & Development (CNP3), College of Pharmacy, University of Florida, Gainesville, Florida 32610, United States

Hendrik Luesch – Department of Medicinal Chemistry, College of Pharmacy and Center for Natural Products, Drug Discovery & Development (CNP3), College of Pharmacy, University of Florida, Gainesville, Florida 32610, United States;

orcid.org/0000-0002-4091-7492

Jay P. McLaughlin – Department of Pharmacodynamics, College of Pharmacy and Center for Natural Products, Drug Discovery & Development (CNP3), College of Pharmacy, University of Florida, Gainesville, Florida 32610, United States

Complete contact information is available at: <https://pubs.acs.org/doi/10.1021/acs.jmedchem.9b01924>

Notes

The authors declare no competing financial interest.

■ ACKNOWLEDGMENTS

The authors acknowledge the University of Florida for support of these initial investigations. In addition, Robert W. Huigens, Ph.D., was supported by a Research Scholar Grant, RSG-18-013-01, CDD, from the American Cancer Society. Research was supported, in part, by the National Institutes of Health, NCI grant (R01CA172310 to H.L.), NCI Research Specialist Award (R50CA211487 to R.R.), and the Debbie and Sylvia DeSantis Chair professorship (H.L.). V.M.N. and A.C.B.-T. are Graduate Fellows at the University of Florida. The National High Magnetic Field Laboratory supported part of our NMR studies at the Advanced Magnetic Resonance Imaging and Spectroscopy (AMRIS) Facility (McKnight Brain Institute;

supported by National Science Foundation Cooperative Agreement No. DMR-1157490 and the State of Florida). X-ray structures were obtained from the Center for X-ray Crystallography at the University of Florida. All high-resolution mass spectra for synthesized analogues were obtained from the University of Florida's Mass Spectrometry Research and Education Center and supported by NIH S10 OD021758-01A1.

ABBREVIATIONS

Avg, average; calcd, calculated; CPP, conditioned place preference; CNBr, cyanogen bromide; Cys, cysteine; DMF, dimethylformamide; GPCR, G protein-coupled receptor; HCRTR2, hypocretin receptor 2; i.c.v., intracerebroventricular; μM , micromolar; nmol, nanomoles; Pro, proline; Val, valine

REFERENCES

- (1) Morone, N. E.; Weiner, D. K. Pain as the fifth vital sign: exposing the vital need for pain education. *Clin. Ther.* **2013**, *35*, 1728–1732.
- (2) Florence, C. S.; Zhou, C.; Luo, F.; Xu, L. The economic burden of prescription opioid overdose, abuse, and dependence in the United States, 2013. *Med. Care* **2016**, *54*, 901–906.
- (3) Vivolo-Kantor, A. M.; Seth, P.; Gladden, R. M.; Mattson, C. L.; Baldwin, G. T.; Kite-Powell, A.; Coletta, M. A. Vital signs: trends in emergency department visits for suspected opioid overdoses – United States, July 2016–September 2017. *Morbidity Mortal. Wkly. Rep.* **2018**, *67*, 279–285.
- (4) Compton, W. M.; Jones, C. M.; Baldwin, G. T. Relationship between nonmedical prescription-opioid use and heroin use. *N. Engl. J. Med.* **2016**, *374*, 154–163.
- (5) CDC/NCHS. *National Vital Statistics System, Mortality*; CDC Wonder, CDC, U.S. Department of Health and Human Services: Atlanta, GA, 2018. <https://wonder.cdc.gov>; <https://www.drugabuse.gov/drugs-abuse/opioids/opioid-overdose-crisis> (accessed June 27, 2019).
- (6) Hwang, C. S.; Janda, K. D. A vision for vaccines: combating the opioid epidemic. *Biochemistry* **2017**, *56*, 5625–5627.
- (7) Muhuri, P. K.; Gfroerer, J. C.; Davies, M. C. *Associations of Nonmedical Pain Reliever Use and Initiation of Heroin Use in the United States*, CBHSQ Data Review; National Survey on Drug Use and Health, 2013.
- (8) Balthaser, B. R.; Maloney, M. C.; Beeler, A. B.; Porco, J. A., Jr.; Snyder, J. K. Remodelling of the natural product fumagillol employing a reaction discovery approach. *Nat. Chem.* **2011**, *3*, 969–973.
- (9) Huigens, R. W., III; Morrison, K. C.; Hicklin, R. W.; Flood, T. A., Jr.; Richter, M. F.; Hergenrother, P. J. A ring distortion strategy to construct stereochemically complex and structurally diverse compounds from natural products. *Nat. Chem.* **2013**, *5*, 195–202.
- (10) Rafferty, R. J.; Hicklin, R. W.; Maloof, K. A.; Hergenrother, P. J. Synthesis of complex and diverse compounds through ring distortion of abietic acid. *Angew. Chem., Int. Ed.* **2014**, *53*, 220–224.
- (11) Morrison, K. C.; Hergenrother, P. J. Natural products as starting points for the synthesis of complex and diverse compounds. *Nat. Prod. Rep.* **2014**, *31*, 6–14.
- (12) Hicklin, R. W.; Lopez Silvia, T. L.; Hergenrother, P. J. Synthesis of bridged oxafenestranes from pleuromutilin. *Angew. Chem., Int. Ed.* **2014**, *53*, 9880–9883.
- (13) Garcia, A.; Drown, B. S.; Hergenrother, P. J. Access to a structurally complex compound collection via ring distortion of the alkaloid sinomenine. *Org. Lett.* **2016**, *18*, 4852–4855.
- (14) Paciaroni, N. G.; Ratnayake, R.; Matthews, J. H.; Norwood, V. M., IV; Arnold, A. C.; Dang, L. H.; Luesch, H.; Huigens, R. W., III A tryptoline ring-distortion strategy leads to complex and diverse biologically active molecules from the indole alkaloid yohimbine. *Chem. – Eur. J.* **2017**, *23*, 4327–4335.
- (15) Tasker, S. Z.; Cowfer, A. E.; Hergenrother, P. J. Preparation of structurally diverse compounds from the natural product lycorine. *Org. Lett.* **2018**, *20*, 5894–5898.
- (16) Charaschanya, M.; Aubé, J. Reagent-controlled regiodivergent ring expansions of steroids. *Nat. Commun.* **2018**, *9*, No. 934.
- (17) Llabani, E.; Hicklin, R. W.; Lee, H.-Y.; Motika, S. E.; Crawford, L. A.; Weerapana, E.; Hergenrother, P. J. Diverse compounds from pleuromutilin lead to a thioredoxin inhibitor and inducer of ferroptosis. *Nat. Chem.* **2019**, *11*, 521–532.
- (18) Zhao, C.; Ye, Z.; Ma, Z. X.; Wildman, S. A.; Blaszczyk, S. A.; Hu, L.; Guizei, I. A.; Tang, W. A general strategy for diversifying complex natural products to polycyclic scaffolds with medium-sized rings. *Nat. Commun.* **2019**, *10*, No. 4015.
- (19) Norwood, V. M., IV; Huigens, R. W., III Harnessing the chemistry of the indole heterocycle to drive discoveries in biology and medicine. *ChemBioChem* **2019**, *20*, 2273–2297.
- (20) O'Connor, S. E.; Maresh, J. J. Chemistry and biology of monoterpene indole alkaloid biosynthesis. *Nat. Prod. Rep.* **2006**, *23*, 532–547.
- (21) Kalaus, G.; Malkieh, N.; Kajtár-Peredy, M.; Brlik, J.; Szabó, L.; Szántay, C. Synthesis of vinca alkaloids and related compounds XXXVI. Preparation of 1-ethyl-1-hydroxyethyl-octahydroindolo[2,3-a]quinolizine derivatives and reactions of their mesylates with cyanide ion. *Heterocycles* **1988**, *27*, 1179–1190.
- (22) Voskressensky, L. G.; Borisova, T. N.; Titov, A. A.; Listratova, A. V.; Kulikova, L. N.; Varlamov, A. V.; Khrustalev, V. N.; Aleksandrov, G. G. Synthesis of azecino[5,4-b]indoles and indolo[3,2-e][2]benzazonines via tandem transformation of hydrogenated indoloquinolizines and indolizines. *Russ. Chem. Bull.* **2012**, *61*, 1231–1241.
- (23) Piemontesi, C.; Wang, Q.; Zhu, J. Enantioselective total synthesis of (-)-terengganensine A. *Angew. Chem., Int. Ed.* **2016**, *55*, 6556–6560.
- (24) Takayama, H.; Misawa, K.; Okada, N.; Ishikawa, H.; Kitajima, M.; Hatori, Y.; Murayama, T.; Wongseripipatana, S.; Tashima, K.; Matsumoto, K.; Horie, S. New procedure to mask the 2,3-pi bond of the indole nucleus and its applications to the preparation of potent opioid receptor agonists with a corynanthe skeleton. *Org. Lett.* **2006**, *8*, 5705–5708.
- (25) Al-Awadhi, F. H.; Gao, B.; Rezaei, M. A.; Kwan, J. C.; Li, C.; Ye, T.; Paul, V. J.; Luesch, H. Discovery, synthesis, pharmacological profiling, and biological characterization of brintonamides A-E, novel dual protease and GPCR modulators from marine cyanobacterium. *J. Med. Chem.* **2018**, *61*, 6364–6378.
- (26) Wills, K. L.; DeVuono, M. V.; Limebeer, C. L.; Vemuri, K.; Makriyannis, A.; Parker, L. A. CB1 receptor antagonism in the bed nucleus of the stria terminalis interferes with affective opioid withdrawal in rats. *Behav. Neurosci.* **2017**, *131*, 304–311.
- (27) Schmeichel, B. E.; Barbier, E.; Misra, K. K.; Contet, C.; Schlosburg, J. E.; Grigoriadis, D.; Williams, J. P.; Karlsson, C.; Pitcairn, C.; Heilig, M.; Koob, G. F.; Vendruscolo, L. F. Hypocretin receptor 2 antagonism dose-dependently reduces escalated heroin self-administration in rats. *Neuropsychopharmacology* **2015**, *40*, 1123–1129.
- (28) Millan, M. J.; Newman-Tancredi, A.; Audinot, V.; Cussac, D.; Lejeune, F.; Nicholas, J. P.; Cogé, F.; Galizzi, J. P.; Boutin, J. A.; Rivet, J. M.; Dekeyne, A.; Gobert, A. Agonist and antagonist actions of yohimbine as compared to fluparoxan at $\alpha(2)$ -adrenergic receptors (AR)s, serotonin (5-HT)(1A), 5-HT(1B), 5-HT(1D) and dopamine D(2) and D(3) receptors. Significance for the modulation of frontocortical monoaminergic transmission and depressive states. *Synapse* **2000**, *35*, 79–95.
- (29) Ghitza, U. E. Overlapping mechanisms of stress-induced relapse to opioid use disorder and chronic pain: clinical implications. *Front. Psychiatry* **2016**, *7*, No. 80.
- (30) Fattore, L.; Fadda, P.; Antinori, S.; Fratta, W. Role of Opioid Receptors in the Reinstatement of Opioid-Seeking Behaviour: An Overview. *Methods in Molecular Biology*; Humana Press: New York, NY, 2015; Vol. 1230, pp 281–293.

- (31) Fattore, L.; Fadda, P.; Zanda, M. T.; Fratta, W. Analysis of Opioid-Seeking Reinstatement in the Rat. *Methods in Molecular Biology*; Humana Press: New York, NY, 2015; Vol. 1230, pp 295–307.
- (32) Orsini, C.; Bonito-Oliva, A.; Conversi, D.; Cabib, S. Susceptibility to conditioned place preference induced by addictive drugs in mice of the C57BL/6 and DBA/2 inbred strains. *Psychopharmacology* **2005**, *181*, 327–336.
- (33) Brabant, C.; Quertemont, E.; Tirelli, E. Influence of the dose and the number of drug-context pairings on the magnitude and the long-lasting retention of cocaine-induced conditioned place preference in C57BL/6J mice. *Psychopharmacology* **2005**, *180*, 33–40.
- (34) Ross, N. C.; Reilly, K. J.; Murray, T. F.; Aldrich, J. V.; McLaughlin, J. P. Novel opioid cyclic tetrapeptides: Trp isomers of CJ-15,208 exhibit distinct opioid receptor agonism and short-acting κ opioid receptor antagonism. *Br. J. Pharmacol.* **2012**, *165*, 1097–1108.
- (35) Eans, S. O.; Ganno, M. L.; Reilly, K. J.; Patkar, K. A.; Senadheera, S. N.; Aldrich, J. V.; McLaughlin, J. P. The macrocyclic tetrapeptide [D-Trp]CJ-15,208 produces short-acting κ opioid receptor antagonism in the CNS after oral administration. *Br. J. Pharmacol.* **2013**, *169*, 426–436.
- (36) Aldrich, J. V.; Senadheera, S. N.; Ross, N. C.; Ganno, M. L.; Eans, S. O.; McLaughlin, J. P. The macrocyclic peptide natural product CJ-15,208 is orally active and prevents reinstatement of extinguished cocaine-seeking behavior. *J. Nat. Prod.* **2013**, *76*, 433–438.
- (37) Yin, J.; Mobarec, J. C.; Kolb, P.; Rosenbaum, D. M. Crystal structure of the human OX2 orexin receptor bound to the insomnia drug suvorexant. *Nature* **2015**, *519*, 247–251.
- (38) Suno, R.; Kimura, K. T.; Nakane, T.; Yamashita, K.; Wang, J.; Fujiwara, T.; Yamanaka, Y.; Im, D.; Horita, S.; Tsujimoto, H.; Tawaramoto, M. S.; Hirokawa, T.; Nango, E.; Tono, K.; Kameshima, T.; Hatsui, T.; Joti, Y.; Yabashi, M.; Shimamoto, K.; Yamamoto, M.; Rosenbaum, D. M.; Iwata, S.; Shimamura, T.; Kobayashi, T. Crystal structures of human orexin 2 receptor bound to the subtype-selective antagonist EMPA. *Structure* **2018**, *26*, 7–19.
- (39) Lancefield, C. S.; Zhou, L.; Lébl, T.; Slawin, A. M. Z.; Westwood, N. J. The synthesis of melohene B and a related natural product. *Org. Lett.* **2012**, *14*, 6166–6169.
- (40) Nemes, A.; Szántay, C.; Czibula, L.; Greiner, I. Synthesis of 18-hydroxyvincamines and epoxy-1,14-secovincamines; a new proof for the aspidospermaneeburnane rearrangement. *Heterocycles* **2007**, *71*, 2347–2362.
- (41) Hugel, G.; Royer, D.; Siguat, F.; Lévy, J. Flow thermolysis rearrangements in the indole alkaloid series: 1,2-dehydroaspidospermidine. *J. Org. Chem.* **1991**, *56*, 4631–4636.
- (42) Wee, A. G. H.; Yu, Q. Asymmetric synthesis of (-)-eburnamnine and (+)-epi-eburnamnine from (4S)-4-ethyl-4-[2-(hydroxycarbonyl)ethyl]-2-butyrolactone. *J. Org. Chem.* **2001**, *66*, 8935–8943.
- (43) Woods, J. R.; Risky, M. V.; Zheng, M. M.; O'Banion, M. A.; Mo, H.; Kirshner, J.; Colby, D. A. Synthesis of 15-methylene-eburnamnine from (+)-vincamine, evaluation of anticancer activity, and investigation of mechanism of action by quantitative NMR. *Bioorg. Med. Chem. Lett.* **2013**, *23*, 5865–5869.
- (44) Ma, Y.; Ge, S.; Wang, W.; Sun, B. Studies on the synthesis, structural characterization, Hirshfeld analysis and stability of apovincamine (API) and its co-crystal (terephthalic acid: apovincamine = 1:2). *J. Mol. Struct.* **2015**, *1097*, 87–97.
- (45) Trojānek, J.; Strouf, O.; Holubek, J.; Čekan, Z. Alkaloids IX. Structure of vincamine. *Collect. Czech. Chem. Commun.* **1964**, *29*, 433–446.
- (46) McLaughlin, J. P.; Marton-Popovici, M.; Chavkin, C. Kappa opioid receptor antagonism and prodynorphin gene disruption block stress-induced behavioral responses. *J. Neurosci.* **2003**, *23*, 5674–5683.
- (47) Aldrich, J. V.; Patkar, K. A.; McLaughlin, J. P. Zyklophin, a systemically active selective kappa opioid receptor peptide antagonist with short duration of action. *Proc. Natl. Acad. Sci.* **2009**, *106*, 18396–18401.
- (48) Bardo, M. T.; Rowlett, J. K.; Harris, M. J. Conditioned place preference using opiate and stimulant drugs: a meta-analysis. *Neurosci. Biobehav. Rev.* **1995**, *19*, 39–51.
- (49) Tzschentke, T. M. Measuring reward with the conditioned place preference paradigm: a comprehensive review of drug effects, recent progress and new issues. *Prog. Neurobiol.* **1998**, *56*, 613–672.
- (50) Huey, R.; Morris, G. M.; Olson, A. J.; Goodsell, D. S. A semiempirical free energy force field with charge-based desolvation. *J. Comput. Chem.* **2007**, *28*, 1145–1152.
- (51) Friesner, R. A.; Banks, J. L.; Murphy, R. B.; Halgren, T. A.; Klicic, J. J.; Mainz, D. T.; Repasky, M. P.; Knoll, E. H.; Shelley, M.; Perry, J. K.; Shaw, D. E.; Francis, P.; Shenkin, P. S. Glide: a new approach for rapid, accurate docking and scoring. 1. Method and assessment of docking accuracy. *J. Med. Chem.* **2004**, *47*, 1739–1749.
- (52) Friesner, R. A.; Murphy, R. B.; Repasky, M. P.; Frye, L. L.; Greenwood, J. R.; Halgren, T. A.; Sanschagrin, P. C.; Mainz, D. T. Extra precision glide: docking and scoring incorporating a model of hydrophobic enclosure for protein-ligand complexes. *J. Med. Chem.* **2006**, *49*, 6177–6196.